AWARD NUMBER: W81XWH-13-1-0449

TITLE: Differential Splicing of Oncogenes and Tumor Suppressor Genes in African- and Caucasian-American Populations: Contributing Factor in Prostate Cancer Disparities?

PRINCIPAL INVESTIGATOR: Norman H Lee, Ph.D.

CONTRACTING ORGANIZATION: George Washington University
Washington, DC 20052

REPORT DATE: October 2015

TYPE OF REPORT: Annual

PREPARED FOR: U.S. Army Medical Research and Materiel Command
Fort Detrick, Maryland 21702-5012

REPORT DOCUMENTATION PAGE

Form Approved
OMB No. 0704-0188

1. REPORT DATE	2. REPORT TYPE	3. DATES COVERED
October 2015	Annual	30 Sep 2014 - 29 Sep 2015

4. TITLE AND SUBTITLE

Differential Splicing of Oncogenes and Tumor Suppressor Genes in African- and Caucasian-American Populations: Contributing Factor in Prostate Cancer Disparities?

5a. CONTRACT NUMBER
W81XWH-13-1-0449

5b. GRANT NUMBER

5c. PROGRAM ELEMENT NUMBER

6. AUTHOR(S)
Norman H Lee, PhD; Bi-Dar Wang, PhD; Jacqueline Olender (PhD graduate student)

E-Mail: nhlee@gwu. edu

5d. PROJECT NUMBER

5e. TASK NUMBER

5f. WORK UNIT NUMBER

7. PERFORMING ORGANIZATION NAME(S) AND ADDRESS(ES)
George Washington University
2300 I Street, NW
Ross Hall
Washington, DC 20037

8. PERFORMING ORGANIZATION REPORT NUMBER

9. SPONSORING / MONITORING AGENCY NAME(S) AND ADDRESS(ES)

U.S. Army Medical Research and Materiel Command
Fort Detrick, Maryland 21702-5012

10. SPONSOR/MONITOR'S ACRONYM(S)

11. SPONSOR/MONITOR'S REPORT NUMBER(S)

12. DISTRIBUTION / AVAILABILITY STATEMENT

Approved for Public Release; Distribution Unlimited

13. SUPPLEMENTARY NOTES

14. ABSTRACT
The overarching goal of this grant award is to characterize differential splicing of oncongenes and tumor suppressor genes in prostate cancer disparities between African American (AA) and Caucasian American (CA) prostate cancer (PCa). In year 1 of this award, we have focused our efforts on two oncogenes, phosphatidylinositol-4,5-bisphosphate 3-kinase catalytic subunit delta (*PIK3CD*) and fibroblast growth factor receptor 3 (*FGFR3*), undergoing population-dependent differential splicing where the AA-specific variants are engendered with a more aggressive oncogenic phenotype *in vitro* and *in vivo.* Full-length cloning of the AA and CA variants of both *PIK3CD* and *FGFR3* have been accomplished. PCa cell lines genetically manipulated to predominantly express the AA-variant of *PIK3CD* or *FGFR3* exhibit greater proliferative and invasive capacity. Detailed analysis of PCa cell lines over-expressing the AA-variant of *PIK3CD* revealed enhanced activation of the PI3K/AKT pathway compared to the same lines over-expressing the CA-variant. Moreover, proliferative capacity of the CA-variant lines was sensitive to inhibition by CAL-101, a small molecule inhibitor designed specifically against PIK3CD. In contrast, proliferative capacity of the AA-variant lines was resistant to CAL-101 inhibition. And these findings (CA variants sensitive and AA variants insensitive to CAL-101) were recapitulated in a xenograft mouse model of proliferation. We are currently testing a xenograft mouse model of metastasis. Year 2 will focus on *in vitro* and *in vivo* characterization of the AA and CA variants of *FGFR3.*

15. SUBJECT TERMS
prostate cancer, cancer health disparities, alternative splicing, African American, European American, oncogenes, tumor suppressor genes

16. SECURITY CLASSIFICATION OF:			17. LIMITATION OF ABSTRACT	18. NUMBER OF PAGES	19a. NAME OF RESPONSIBLE PERSON
a. REPORT	b. ABSTRACT	c. THIS PAGE			USAMRMC
Unclassified	Unclassified	Unclassified	Unclassified	30	19b. TELEPHONE NUMBER *(include area code)*

Table of Contents

1. INTRODUCTION

There are striking population/race disparities in prostate cancer (PCa) risk and survival outcome borne out of current health statistics data. This is particularly evident between African Americans (AA) and their European American (EA) counterparts. Epidemiologic studies have shown that higher mortality and recurrence rates for prostate cancer are still evident in AA men even after adjustment for socioeconomic status, environmental factors and health care access. Thus, it is likely that intrinsic biological differences account for some of the cancer disparities. Our overarching hypothesis is that the biological component of prostate cancer health disparities is due, in part, to population-dependent differential splicing of oncogenes and tumor suppressor genes in cancer specimens. The application of genomic approaches has identified splice variants in AA specimens, but absent in EA specimens, encoding more aggressive oncogenic proteins, thereby producing a more cancerous phenotype.

2. KEYWORDS

Prostate cancer, cancer health disparities, alternative RNA splicing, African American, European American, oncogenes, tumor suppressor genes, phosphatidylinositol-4,5-bisphosphate 3-kinase catalytic subunit delta, fibroblast growth factor receptor 3

3. ACCOMPLISHMENTS

Year 2 goals as stated in SOW:

Specific Aim 1. To define splice variant pairs (AA-specific variant versus EA-counterpart variant) associated with differential oncogenic behavior *in vitro*, and to delineate the mechanism of action.

Task 1. **Full-length cloning and *in vitro* validation of splice variant pairs**. Subtasks will be run concurrently and are as follows:

1a. Full-length cloning of splice variant pairs and ectopic over-expression into PCa cell lines.

1b. *In vitro* validation of differential oncogenic behavior by full-length splice variant pairs. Splice variant pairs (e.g. AA-specific versus EA-counterpart variant of PIK3CD and FGFR3) will be individually over-expressed in the same PCa cell line background, and screened for differential oncogenic behavior.

1c. *In vitro* validation of differential protein/enzyme activity by full-length splice variant pairs. Splice variant pairs will be individually over-expressed into appropriate cell line for enzyme activity assays and/or assessment of downstream activation of cell signaling components. Activation of downstream signaling components by splice variants will be assessed, for example, by measuring phosphorylation of downstream signaling components with phospho-specific antibodies (e.g. phospho-Akt, phospho-ERK, etc.).

Task 2. ***In vitro* screening and full-length cloning of additional splice variant pairs**. Subtasks will be run concurrently and are as follows:

2a. Exon-targeting and splice junction-targeting siRNAs will be used in appropriate PCa cell lines to identify splice variant pairs exhibiting differential oncogenic behavior following knockdown.

2b. From subtask 2a, we will select 5-10 splice variant pairs that exhibited differential oncogenic behavior for full-length cloning and ectopic over-expression in appropriate cell lines.

2c. Cell lines over-expressing individual full-length variant pairs (e.g. AA-specific variant versus EA-counterpart variant) will be validated *in vitro* for differential oncogenic behavior using *in vitro* screens described in subtask 1b. We will also test for differential sensitivity of splice variant pairs to small molecule inhibitors, if available.

2d. Cell lines over-expressing individual variant pairs (e.g. AA-specific variant versus EA-counterpart variant) will be screened *in vitro* for differential protein/enzyme activity and cell signaling as described in subtask 1c. We will also test for differential sensitivity of splice variant pairs to small molecule inhibitors, if available.

Specific Aim 2. To characterize oncogenic differences of splice variant pairs *in vivo* using xenograft animal models.

Task 1. **Validate differential oncogenic behavior of the splice variant pair for PIK3CD *in vivo***. Stably expressed S (AA-specific) or L variants (EA-counterpart) of *PIK3CD* in appropriate cell line(s) will be transplanted ($1x10^6$ to 10^7 cells) into male SCID-NOD immuno-deficient mice for proliferation and metastasis assays.

Task 2. **Validate differential oncogenic behavior of additional splice variant pairings *in vivo.*** We will test *in vivo* an additional 4-9 splice variant pairings defined in Aim 1, Task 1, Subtasks 1b-1c (e.g. one variant pairing could be the AA-specific and EA-counterpart variants for *FGFR3*), or defined in Aim 1, Task 2, Subtasks 2c-2d.

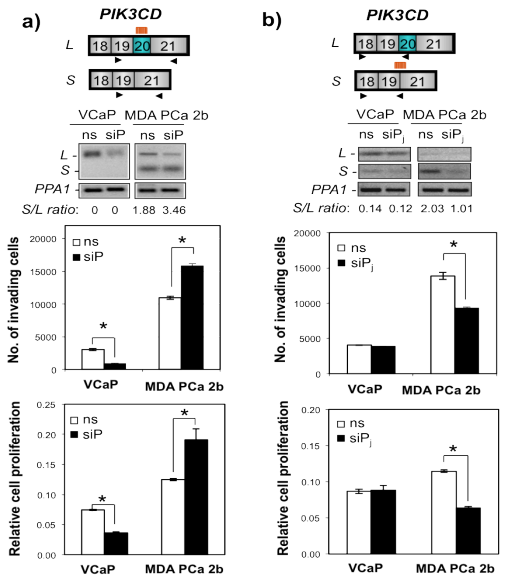

Fig. 1. Functional consequences of targeted knockdown of splice variants of PIK3CD in AA and EA PCa cell lines. (a) Effects of siRNA-mediated knockdown of PIK3CD long splice variant (L) found in EA PCa cell line VCaP and AA PCa cell line MDA PCa 2b. **(b)** Effects of siRNA-mediated knockdown of PIK3CD short splice variant (S) found in AA PCa cell line MDA PCa 2b. EA PCa cell line VCaP expresses very little to no S variant. Knockdown of L variant was accomplished with an exon 20-specific siRNA, while knockdown of S variant was accomplished by an siRNA spanning exons 19 and 21. **(c)** Effects of siRNA-mediated knockdown of PIK3CD long splice variant (L) in MDA PCa 2b. Data are the mean ± SE of 4 independent experiments.

Year 2 major accomplishments include the following:

i. **Manuscript detailing our findings on the oncogenic behavior of the AA-specific/enriched *PIK3CD* short variant (*PIK3CD-S*) compared to the EA *PIK3CD* long variant (*PIK3CD-L*).**

We have completed our *in vitro* and *in vivo* studies comparing the S and L variants of PI3KCD. The manuscript is being drafted and we anticipate submission within the next 1-2 months. Our plan is to submit the manuscript to *Nature Communications*. Findings can be summarized as follows:

PIK3CD-S exhibits a more aggressive cancer phenotype compared to PIK3CD-L. We demonstrate that the S variant for PIK3CD encodes a

more aggressive version of the gene (i.e. leading to greater proliferation and invasion of cancer cells) compared to the L variant counterpart. SiRNA-mediated knockdown of the L variant in EA PCa cell line VCaP leads to a decrease in Matrigel invasion and a decrease in proliferation as assessed by BrdU incorporation (**Fig. 1A**). By comparison, the AA PCa cell line MDA PCa 2b expresses both L and S variants, and knockdown of the L variant leads to predominant expression of the S variant and a corresponding increase in Matrigel invasion and increase in proliferation (**Fig. 1A**). Next, we investigated S variant knockdown. VCaP cells express little to no S variant; hence, targeted siRNA-mediated knockdown of this variant led to no change in Matrigel invasion and proliferation (**Fig. 1B**). In contrast, targeted knockdown of the S variant in MDA PCa 2b cells leads to decreased Matrigel invasion and decreased proliferation (knockdown of S variant leads to predominant expression of L variant) (**Fig. 1B**). These data indicate that the overall S to L ratio in MDA PCa 2b cells dictates the oncogenic profile of this AA PCa cell line. Namely, knocking down the L variant in MDA PCa 2b cells increases the S/L ratio, leading to a higher proportion of the aggressive S variant and consequently increased invasiveness and proliferation of the cell line. Of interest, the increase in invasion and proliferation was accompanied by an increase in phosphorylation (i.e. activation) of downstream signaling components of PI3KCD, namely AKT, mTOR and ribosomal protein S6 (**Fig. 1C**). On the other hand, knocking down the S variant in MDA PCa 2b cells decreases the S/L ratio, leading to a higher proportion of the less aggressive L variant and consequently decreased invasiveness and proliferation of the cell line.

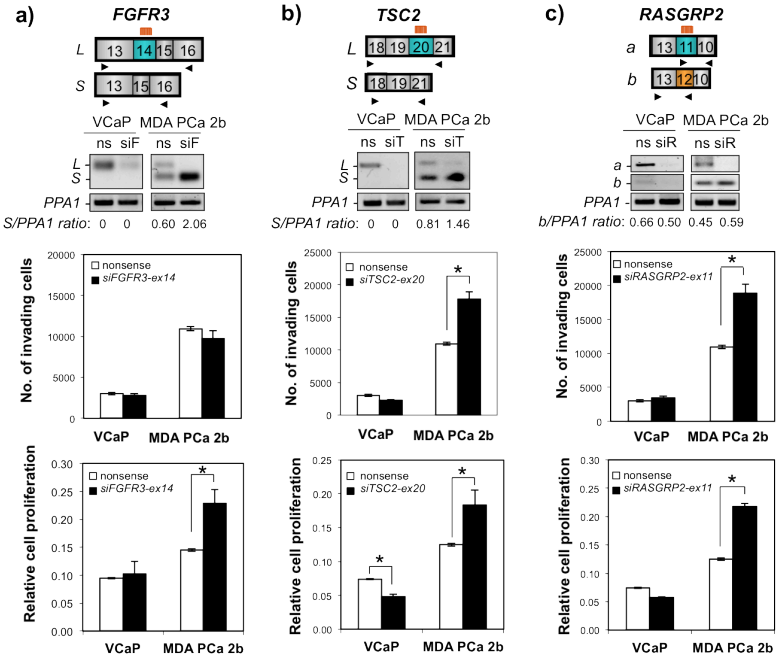

FIGURE 2. Functional consequences of targeted knockdown of splice variants of PIK3CD in AA and CA PCa cell lines. **(a)** Effects of siRNA-mediated knockdown of PIK3CD long splice variant (L) found in CA PCa cell line VCaP and AA PCa cell line MDA PCa 2b. The L variant is found expressed in both VCaP and MDA PCa 2b cells. **(b)** Effects of siRNA-mediated knockdown of PIK3CD short splice variant (S) found in AA PCa cell line MDA PCa 2b. The EA PCa cell line VCaP expresses very little to no S variant. Knockdown of the L variant was accomplished with an exon 20-specific siRNA, while knockdown of the S variant was accomplished by an siRNA spanning exons 19 and 21. **(c)** Effects of siRNA-mediated knockdown of FGFR3 long splice variant (L) found in CA PCa cell line VCaP and AA PCa cell line MDA PCa 2b. The L variants are found expressed in both VCaP and MDA PCa 2b cells. Data are the mean ± SE of 4-8 independent experiments.

AA-specific/enriched variants of FGFR3, TSC2 and RASGRP2 exhibit a more oncogenic phenotype compared to corresponding EA variants. We demonstrate an analogous increased proliferative and/or invasive behavior in MDA PCa 2b cells when the AA-specific/enriched variant (found exclusively or nearly exclusively in AA cell lines) to EA-counterpart variant

(found in both EA and AA cell lines) ratio was increased for fibroblast growth factor receptor 3 (FGFR3), tuberous Sclerosis 2 (TSC2) and RAS guanyl-releasing protein 2 (RASGRP2) (**Fig. 2A-C**).

AA-specific/enriched variant PI3KCD-S is resistant to small molecule inhibitor CAL-101, while EA variant PI3KCD-L is sensitive. We demonstrate that the more aggressive invasive behavior observed in the AA PCa cell line MDA PCa 2b upon increasing the S/L variant ratio was associated with an augmented activation of the PI3K/AKT pathway. This was evidenced by the increased phosphorylation of AKT at amino acids Thr308 and Ser473, mTOR and ribosomal protein S6 (S6) (**Fig. 3A**). We subsequently stably over-expressed the PIK3CD-S and PIK3CD-L variants (individually in the EA PCa cell lines PC-3 and VCaP. These stably transfected cell lines were tested *in vitro* for sensitivity to CAL-101 treatment (**Figure 3B**). CAL-101 is a PIK3CD inhibitor in clinical trials for various cancers. PCa cell lines over-expressing the EA PIK3CD-L variant exhibited a decrease in the activity of the PI3K/AKT pathway following CAL-101 treatment, as seen by a loss of AKT, mTOR and S6 phosphorylation. Remarkably, the same EA PCa cell lines stably over-expressing equivalent levels of the AA PIK3CD-S variant were completely resistant to CAL-101. In other words, there was no significant change in AKT, mTOR and S6 phosphorylation levels before and after CAL-101 treatment.

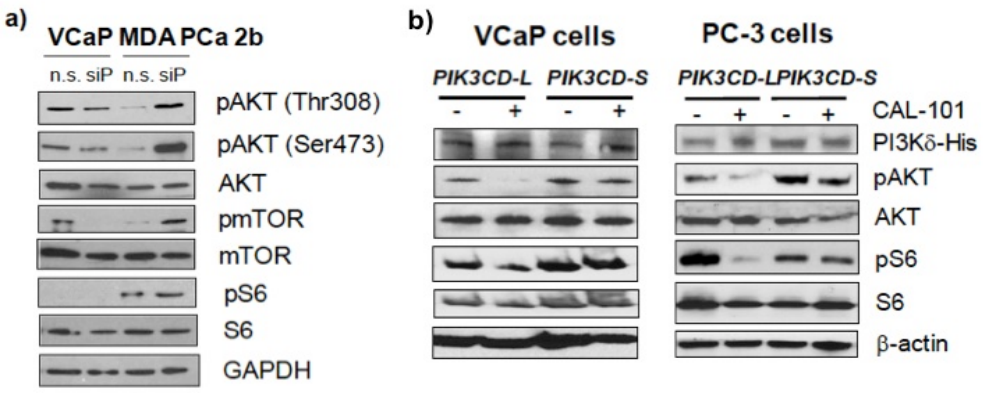

Fig 3. SiRNA-mediated knockdown or pharmacological inhibition reduces activity of the PI3K/AKT signaling in PIK3CD-L- but not in PIK3CD-S-expressing cells. (a) EA VCaP and AA MDA PCa 2b cells were transfected with nonsense siRNA (n.s.) or siRNA against exon 20 of PIK3CD-L (siP). Western blot analysis revealed that siP knockdown caused a decrease in the phosphorylation status (i.e. activation) of AKT (pAKT), mTOR (pmTOR) and S6 (pS6) in VCaP cells, while siP transfection increased phosphorylation of these signaling proteins in MDA PCa 2b. **(b)** Phosphorylation status of AKT, mTOR and S6 proteins are inhibited by CAL-101 in VCaP and PC-3 cells over-expressing the PIK3CD-L variant but not the PIK3CD-S variant. Data are the mean ± SE of 4 independent experiments.

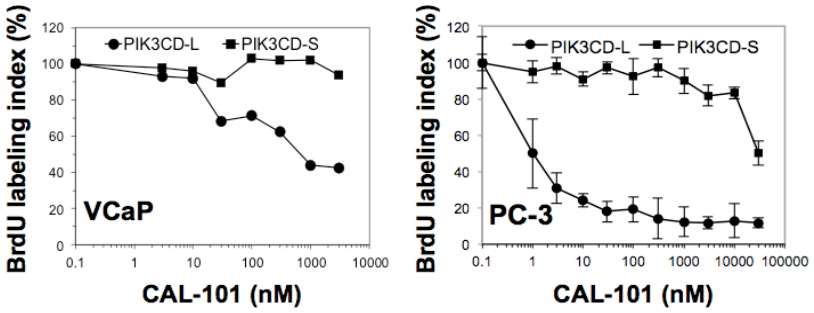

Fig. 4. CAL-101 treatment inhibits proliferation of PIK3CD-L- but not in PIK3CD-S-expressing VCaP (left panel) and PC-3 cells (right panel). Data are the mean ± SE of 4-6 independent experiments.

In cell proliferation assays, we demonstrate that BrdU labeling in VCaP and PC-3 cells over-expressing the EA PIK3CD-L variant was inhibited by CAL-101 in a dose-dependent manner, while proliferation of VCaP and PC-3 cells over-expressing the AA PIK3CD-L variant were resistant to CAL-101 (**Fig. 4**).

Cell-free system: PI3KCD-S activity is resistant to CAL-101, while EA variant PI3KCD-L is sensitive. We have recently purified His-tagged PIK3CD-S and -L using a HisPur Ni-NTA column approach (**Fig. 4A**), and subjected the purified proteins to a cell-free *in vitro* colorimetric-based PI3K activity/inhibitor assay (**Fig. 4B**). Interestingly, baseline activities of the S and L isoforms were not significantly different. Notwithstanding, our results clearly demonstrate that the S isoform was resistant to inhibition by CAL-101 and wortmannin, whereas L isoform activity was completely inhibited by these small molecule inhibitors.

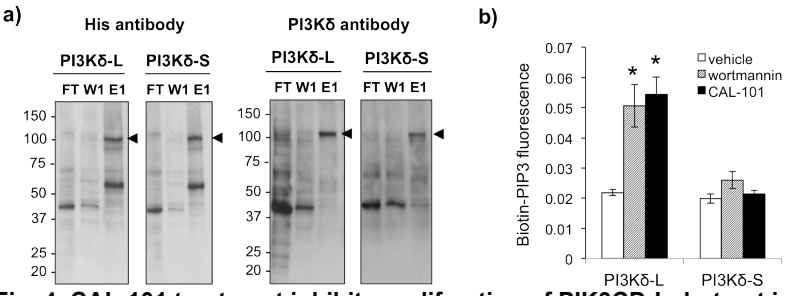

Fig. 4. CAL-101 treatment inhibits proliferation of PIK3CD-L- but not in PIK3CD-S-expressing VCaP (left panel) and PC-3 cells (right panel). Data are the mean + SE of 4-6 independent experiments.

Xenograft of PC-3 cells over-expressing PIK3CD-S is resistant, while PC-3 over-expressing PIK3CD-L is sensitive, to the anti-proliferative and anti-metastatic effects of CAL-101.

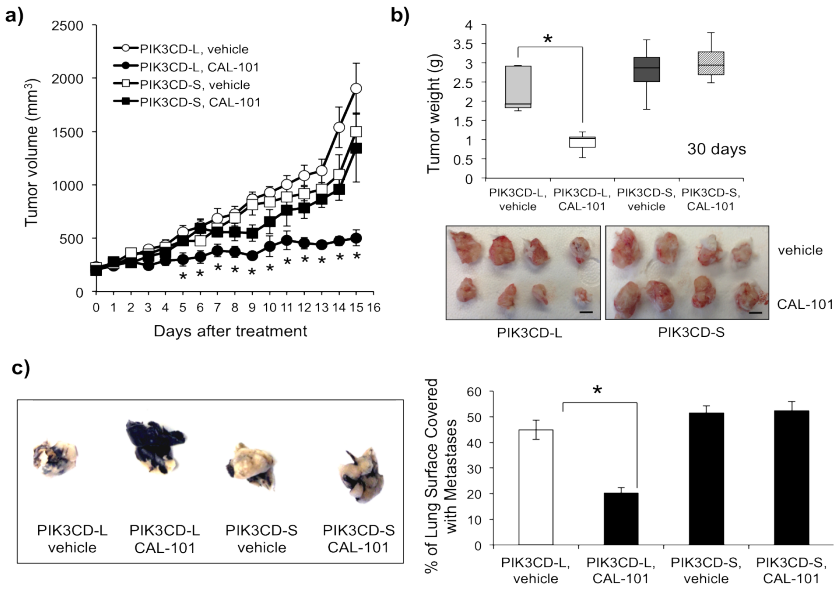

Fig. 5. Differential response of *PI3KCD-L* and *PI3KCD-S* isoforms to CAL-101 treatment *in vivo*. (**a**) PC-3 cells stably expressing *PIK3CD-L* exhibited reduced tumorigenesis in NOD-SCID mice upon CAL-101 treatment. In contrast, PC-3 cells stably expressing *PIK3CD-S* exhibited resistance to CAL-101 inhibition of tumorigenesis in NOD-SCID mice. Two million PC-3 cells expressing *PIK3CD-L* or *PIK3CD-S* were injected subcutaneously into the left flanks of each NOD-SCID mice and allowed to develop tumors under vehicle or CAL-101 treatment. The data represent the mean tumor size ± SEM, with * $P < 0.05$ (ANOVA, n=10 independent mice for each treatment group at each time point). (**b**) Tumor weights and gross morphology of the tumor xenografts from (**a**). The box plots represent mean tumor weights after 15-days vehicle or CAL-101 treatment (ANOVA, n=5 independent mice for each treatment group at each time point). (**c**) Intravenous tail vein with 10^5 PC-3 cells ectopically expressing *PIK3CD*-S or *PIK3CD*-L for lung metastasis assay. Animals treated with daily IP injections of vehicle (veh), PC-3 cells expressing either variant grew and metastasized robustly. Animals treated with daily IP injections of CAL-101 (CAL; 25 mg/kg), cells expressing S variant still exhibited robust growth and metastasis, while L expressing cells exhibited significant inhibition of growth and metastasis. (*P<0.05, significantly different from vehicle treated cells expressing L; ANOVA with post-hoc test). n=10 for each exp. group. Representative xenograft growths and metastases (white masses).

We demonstrate in a xenograft mouse model that growth of PC-3 cells over-expressing the AA-specific/enriched PIK3CD-S variant were resistant to the inhibitory effects of CAL-101. By comparison, PC-3 cells over-expressing the EA PIK3CD-L variant were particularly sensitive to CAL-101 treatment (**Fig. 5**).

Molecular modeling of PIK3CD-S and -L protein variants. Molecular modeling demonstrates that CAL-101 is unable to dock onto the ATP binding pocket of PIK3CD-S due to the absence of key amino acids Glu826 and Val828 (these amino acids are encoded by exon 20 that is missing in PIK3CD-S), whereas CAL-101 efficiently docks and consequently would inhibit kinase activity of PIK3CD-L (**Fig. 6**). These findings provide an explanation for the resistance of PIK3CD-S to small molecule inhibitors. We anticipate that future studies will be aimed at developing inhibitors specific to PIK3CD-S.

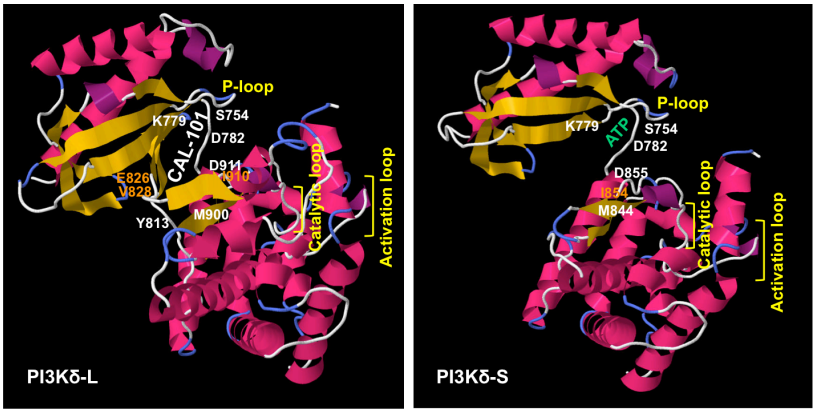

Fig. 6. Molecular modeling of CAL-101 docking to PIK3CD-L but not to PIK3CD-S.

Year 2 opportunities for training and professional development:

Year 2 of this proposal has continued to provide hands-on training for PhD graduate student Jacqueline Olender. The PI is serving as Ms. Olender's mentor and she has participated in both the *in vitro* and *in vivo* work described herein. This work is part of Ms. Olender's PhD dissertation research project.

Dissemination of results and outreach to communities of interest:

During Year 2 of this grant, we had two year 1 medical students (MS1) rotate into our laboratory (2-4 days per week). MS1 students have participated in experiments under the supervision of myself and Dr. Wang.

Year 3 goals:

i. Fully characterize the AA FGFR3-S and EA FGFR3-L splice variants using the same *in vitro* and *in vivo* approaches outlined in our results section for PIK3CD. We have cloned both S and L variants, and we are in the process of stably expressing these variants ectopically in PCa cell lines.

ii. Begin molecular studies to understand the mechanism of differential splicing in AA versus EA PCa for the PI3KCD and FGFR3 variants. This is a fundamental question that needs to be addressed. We envision this work to be the basis of our future inquiries in

cancer disparities research, and we have recently submitted 2015 grant to DOD detailing our proposed experiments to ascertain mechanism.

4. IMPACT

Impact on the development of the principal discipline(s) of the project:

Principal discipline -- Understanding prostate cancer biology and disparities. Taken together, our *in vitro* and *in vivo* findings with the EA PIK3CD-L and AA PIK3CD-S variants provide evidence that differential splicing may play a critical role in PCa health disparities. Our future goal is to identify additional population-specific oncogene variants (i.e. FGFR3 which we are currently working on) that exhibit differential oncogenic behavior and/or sensitivity to small molecule inhibitors, thereby further supporting our hypothesis.

Impact on other disciplines:

Other disciplines -- Cancer chemoresistance. Our results in Year 2 demonstrate conclusively that the AA PIK3CD-S variant protein, but not the EA PIK3CD-L variant protein, is resistant to CAL-101, a small molecule inhibitor that has been specifically designed to inhibit PIK3CD and this inhibitor is undergoing clinical trials for treatment of hematological cancers. Our conclusions are based on the following complimentary approaches: i) *in vitro* culture of PCa cell lines that have been genetically manipulated (i.e. siRNA-mediated knockdown), ii) xenograft studies investigating both proliferation and metastasis, and iii) most recently, a cell-free system to study the recombinant purified protein variants. Taken together, our findings have potential important clinical implications as it relates to population-specific differential splicing of oncogenes and primary chemoresistance.

Impact on technology transfer:

Our findings that the AA PIK3CD-S variant protein is resistant to CAL-101 has sparked interests in companies that are investigating small molecule inhibitors of kinases involved in cancer progression. These companies are gaining an appreciation that alternative splicing in kinases can affect the sensitivity these signaling proteins to cancer therapeutic agents. Our findings raise the issue related to prescreening patients for their variant protein in order to prognosticate whether a particular therapeutic agent will be efficacious in treating the cancer. We are in continued discussions with companies such as Celdara Medical (Lebanon, CT; http://www.celdaramedical.com/) concerning the leveraging of our findings.

Impact on society beyond science and technology:

Nothing to report

5. CHANGES/PROBLEMS

Changes in approach:

None

Actual or anticipated problems or delays:

None

Changes that had significant impact on expenditures:

None

Significant changes in use or care of human subjects, vertebrate animals, biohazards, and/or select agents:

None

6. PRODUCTS

Publications, conference papers, and presentations:

i. Wang B.-D., Ceniccola K., Yang Q., Andrawis R., Patel V., Ji Y., Rhim J., Olender J., Popratiloff A., Latham P., Patierno S.R. and Lee N.H. (2015) Identification and functional validation of reciprocal microRNA-mRNA pairings in African American prostate cancer disparities. ***Clinical Cancer Research,*** DOI: 10.1158/1078-0432.CCR-14-1566. Part of the published work was supported by W81XWH-13-1-0449. Our gene expression analysis provided gene level data as well as alternative splicing data. The former data was used in the ***Clinical Cancer Research*** article, while the latter data will be used for our upcoming manuscript described in iii. See appendix for published manuscript.

ii. Write-up on our published work (Clinical Cancer Research, DOI: 10.1158/1078-0432.CCR-14-1566) appeared in ***Nature Reviews Urology,*** DOI: 10.1038/nrurol.2015.161 (see appendix).

iii. We are in the process of drafting a manuscript on our findings with PI3KCD-S and -L variants. Submission of our manuscript is anticipated in 1-2 months to *Nature Communications*.

Website(s) or other Internet site(s):

None

Technologies or techniques:

None

Inventions, patent applications, and/or licenses:

i. A provisional patent application has been filed. Application number: 61/948,218. Filing date: 3/5/2014. Application title: Companion Diagnostics for Cancer and Screening Methods to Identify Companion Diagnostics for Cancer Based on Splicing Variants

Other Products:

None

7. PARTICIPANTS & OTHER COLLABORATORS

Individuals working on this project:

Name:	Norman H Lee, PhD
Project Role:	PI
Nearest person month worked:	3
Contribution to project:	Direct and oversee entire project. Involved in experimental design and statistical analysis.

Name:	Bi-Dar Wang, PhD
Project Role:	Co-Investigator
Nearest person month worked:	3
Contribution to project:	Contributed to the cloning of variant cDNAs, in vitro, xenograft assays and cell-free protein purification and analysis.
Funding support:	Partially supported by GWU bridge support

Name:	Jacqueline Olender
Project Role:	PhD graduate student
Nearest person month worked:	12
Contribution to project:	Contributed to the cloning of variant cDNAs, in vitro and in vivo assays

Name:	Patricia Latham, MD
Project Role:	Co-Investigator
Nearest person month worked:	1
Contribution to project:	Animal necropsy and immunohistochemistry of xenografts

Change in the active other support of the PD/PI(s) or senior/key personnel since the last reporting period:

None

Other organizations were involved as partners:

Nothing to report

8. SPECIAL REPORTING REQUIREMENTS

Nothing to report

9. APPENDICES

i. Wang B.-D., Ceniccola K., Yang Q., Andrawis R., Patel V., Ji Y., Rhim J., Olender J., Popratiloff A., Latham P., Patierno S.R. and Lee N.H. (2015) Identification and functional validation of reciprocal microRNA-mRNA pairings in African American prostate cancer disparities. ***Clinical Cancer Research,*** DOI: 10.1158/1078-0432.CCR-14-1566. Part of the published work was supported by W81XWH-13-1-0449.

ii. Write-up on our published work (Clinical Cancer Research, DOI: 10.1158/1078-0432.CCR-14-1566) appeared in ***Nature Reviews Urology,*** DOI: 10.1038/nrurol.2015.161.

Published OnlineFirst June 18, 2015; DOI: 10.1158/1078-0432.CCR-14-1566

Clinical Cancer Research

Identification and Functional Validation of Reciprocal microRNA–mRNA Pairings in African American Prostate Cancer Disparities

Bi-Dar Wang[1], Kristin Ceniccola[1], Qi Yang[1], Ramez Andrawis[2], Vyomesh Patel[3], Youngmi Ji[4], Johng Rhim[5], Jacqueline Olender[1], Anastas Popratiloff[6], Patricia Latham[7], Yinglei Lai[8], Steven R. Patierno[9,10], and Norman H. Lee[1]

Abstract

Purpose: African Americans (AA) exhibit higher rates of prostate cancer incidence and mortality compared with European American (EA) men. In addition to socioeconomic influences, biologic factors are believed to play a critical role in prostate cancer disparities. We investigated whether population-specific and -enriched miRNA–mRNA interactions might contribute to prostate cancer disparities.

Experimental Design: Integrative genomics was used, combining miRNA and mRNA profiling, miRNA target prediction, pathway analysis, and functional validation, to map miRNA–mRNA interactions associated with prostate cancer disparities.

Results: We identified 22 AA-specific and 18 EA-specific miRNAs in prostate cancer versus patient-matched normal prostate, and 10 "AA-enriched/-depleted" miRNAs in AA prostate cancer versus EA prostate cancer comparisons. Many of these population-specific/-enriched miRNAs could be paired with target mRNAs that exhibited an inverse pattern of differential expression. Pathway analysis revealed EGFR (or ERBB) signaling as a critical pathway significantly regulated by AA-specific/-enriched mRNAs and miRNA–mRNA pairings. Novel miRNA–mRNA pairings were validated by qRT-PCR, Western blot, and/or IHC analyses in prostate cancer specimens. Loss/gain of function assays performed in population-specific prostate cancer cell lines confirmed miR-133a/*MCL1*, miR-513c/*STAT1*, miR-96/*FOXO3A*, miR-145/*ITPR2*, and miR-34a/*PPP2R2A* as critical miRNA–mRNA pairings driving oncogenesis. Manipulating the balance of these pairings resulted in decreased proliferation and invasion, and enhanced sensitization to docetaxel-induced cytotoxicity in AA prostate cancer cells.

Conclusion: Our data suggest that AA-specific/-enriched miRNA–mRNA pairings may play a critical role in the activation of oncogenic pathways in AA prostate cancer. Our findings also suggest that miR-133a/*MCL1*, miR-513c/*STAT1*, and miR-96/*FOXO3A* may have clinical significance in the development of novel strategies for treating aggressive prostate cancer. *Clin Cancer Res; 1–15. ©2015 AACR.*

[1]Department of Pharmacology and Physiology, The George Washington University School of Medicine and Health Sciences, Washington, District of Columbia. [2]Medical Faculty Associates, The George Washington University School of Medicine and Health Sciences, Washington, District of Columbia. [3]Oral and Pharyngeal Cancer Branch, National Institute of Dental and Craniofacial Research, NIH, Bethesda, Maryland. [4]Cartilage Biology and Orthopedics Branch, National Institute of Arthritis and Musculoskeletal and Skin Diseases, NIH, Bethesda, Maryland. [5]Department of Surgery, Center for Prostate Disease Research, Uniformed Services University of the Health Sciences, Bethesda, Maryland. [6]Department of Anatomy and Regenerative Biology, The George Washington University School of Medicine and Health Sciences, Washington, District of Columbia. [7]Department of Pathology, The George Washington University School of Medicine and Health Sciences, Washington, District of Columbia. [8]Department of Statistics, The George Washington University, Washington, District of Columbia. [9]GW Cancer Institute, The George Washington University Medical Center, Washington, District of Columbia. [10]Duke Cancer Institute, Duke University Medical Center, Durham, North Carolina.

Note: Supplementary data for this article are available at Clinical Cancer Research Online (http://clincancerres.aacrjournals.org/).

Corresponding Author: Norman H. Lee, George Washington University School of Medicine and Health Sciences, 2300 I Street North West, Washington, DC 20037. Phone: 202-994-8855; Fax: 202-994-2870; E-mail: nhlee@gwu.edu

doi: 10.1158/1078-0432.CCR-14-1566

Introduction

MiRNAs (miRNAs) are small regulatory RNAs of approximately 21 to 25 nucleotides in length that complementarily target mRNAs to inhibit translation and/or promote mRNA degradation. Recently, several reports have suggested that miRNA aberrations may be an important factor in cancer development (1, 2). The potential connection between miRNA regulation and cancer has been made at several levels, suggesting that miRNAs play critical roles in cellular growth and differentiation, which are two cellular processes commonly defective in tumor cells (3). Additional evidence for the involvement of miRNAs in human cancer comes from observations that approximately 50% of these small regulatory RNAs are transcribed from genomic regions associated with a loss of heterozygosity, minimal amplicons, or breakpoint cluster regions (4). Cancer-related miRNAs have been identified in various cancers (5). In general, oncogenic miRNAs upregulated in tumors act as oncogenes (repressing tumor-suppressor and apoptosis-associated genes), whereas tumor-suppressor miRNAs are downregulated (leading to derepression of oncogenes and proliferation-related genes; ref. 6). Although many miRNAs are differentially expressed in various cancers, the identity of the mRNAs specifically targeted by these miRNAs, functional

Published OnlineFirst June 18, 2015; DOI: 10.1158/1078-0432.CCR-14-1566

Translational Relevance

Prostate cancer tends to be more aggressive and lethal in African Americans (AA) compared with European Americans (EA). An understanding of the molecular mechanisms associated with prostate cancer disparities can aid in the development of innovative and improved therapeutic options for the AA population. Integrative functional genomics analysis of patient specimens and prostate cancer cell lines has identified novel AA-specific and -enriched miRNA–mRNA pairs, including miR-133a/*MCL1*, miR-513c/*STAT1*, miR-96/*FOXO3A*, miR-145/*ITPR2*, and miR-34a/*PPP2R2A*, that reside in key oncogenic signaling pathways. The presence of these miRNA–mRNA pairs is computationally predicted to augment activation of EGFR–PI3K–AKT signaling in AA compared with EA cancers. Specific manipulation of these pairs reduced cell proliferation/invasion and enhanced docetaxel-induced cytotoxicity in AA prostate cancer cell lines. Converse manipulation resulted in a more aggressive phenotype in EA cell lines. Thus, targeting these novel miRNA–mRNA pairs may provide a potential clinical strategy for reducing AA prostate cancer burden.

consequences of miRNA–mRNA pairings and their contributions to cancer pathogenesis remain to be elucidated.

Prostate cancer is now the most frequently diagnosed cancer and the second most common cause of cancer-related deaths in men residing in the United States (7). AAs have among the highest incidence of prostate cancer and mortality attributable to this disease, being 1.6 times more likely to develop prostate cancer, and 2.4 times more likely to die from prostate cancer compared with their EA counterparts (8). Multiple socioeconomic and environmental factors have been postulated to explain the observed prostate cancer health disparities, such as access to care, attitudes toward health care, socioeconomic differences, diet, and differences in the type and aggressiveness of treatment (8). However, adjustment for these factors does not preclude the higher mortality and recurrence rate in AA men and suggests that intrinsic biologic differences exist (9). The application of epidemiology and genomics has revealed biologic factors implicated in prostate cancer health disparities between AA and EA, such as differences in the hormonal milieu of the tumor (10), oncogenic activation (11), and tumor immunobiology (12). More recently, our genomic analysis identified multiple signaling pathways converging on the androgen receptor (AR) to activate transcription of AR-target genes promoting prostate cancer progression and aggressiveness in AA patients (13).

Given the importance of miRNAs in cancer, studies have been forthcoming on the association of miRNAs in prostate cancer pathogenesis. Volinia and colleagues (1) performed large-scale analysis of miRNA expression profiles in 540 samples derived from six types of solid tumors, and demonstrated that 46 miRNAs were differentially expressed when comparing prostate cancer with patient-matched normal prostate (NP), including upregulated let-7d*, miR-17-5p, and miR-21, and downregulated miR-24, miR-29, and miR-128a. An miRNA profiling study by Ozen and colleagues (14) revealed that 76 of the 85 differentially expressed miRNAs were downregulated (such as let-7c, miR-145, and miR-125b) in the prostate cancer clinical samples compared with normal tissues. More recently, Wang and colleagues (15) identified a set of deregulated miRNAs associated with cell-cycle regulation in aggressive prostate cancer by combining miRNA expression profiling and coexpression network analysis. Although these profiling studies have begun to shed light on the involvement of miRNAs in prostate cancer development, questions on the role of miRNAs in prostate cancer disparities still remain. A recent study evaluated the impact of miRNAs contained in the region of 8q24, a genetic risk locus conferring prostate cancer in AAs. However, no empirical evidence of miRNA transcription was found within the 8q24 prostate cancer risk locus (16). In the present study, we applied a systems biology approach, by combining genome-wide miRNA and mRNA expression profiling in prostate cancer patient specimens, miRNA target predictions, and miRNA–mRNA pairing and pathway analyses, to identify the oncogenic signaling pathway most significantly regulated by AA-specific/-enriched mRNAs and miRNA–mRNA pairings. The AA-specific/-enriched miRNA and mRNA elements were also evaluated in AA and EA prostate cancer cell lines for their functional relevance in cell proliferation, invasion, and chemosensitivity to cytotoxic agents.

Materials and Methods

Acquisition and characteristics of prostate cancer clinical specimens

Tissues were procured from the George Washington University Medical Faculty Associates adhering to IRB approved protocols (IRB#020867), as detailed in Supplementary Materials and Methods. High-quality prostate cancer and patient-matched NP biopsy cores from each of 20 AA and 15 EA patients were collected and processed for the microarray analyses. Prostate cancer cores were determined by pathologist to have Gleason score of 6 to 7 (17 AA and 13 EA) or 8to 9 (3 AA and 2 EA), whereas NP cores were negative for cancer. There was no significant difference between the two racial groups with respect to age (average age for AAs was 62.3 ± 8.2, average age for EAs was 63.3 ± 9.2) and Gleason score (Supplementary Table S1A).

Prostate cancer cell lines

Prostate cancer cell lines were purchased from the ATCC and passaged less than 6 months after receipt/resuscitation. Cell lines were tested and authenticated at the ATCC by short tandem repeat profiling of multiple unique genetic loci (D5S818, D13S317, D7S820, D16S539, vWA, TH01, Amelogenin, TPOX, and CSF1PO).

Gene-expression microarrays

Total RNA was isolated from prostate cancer and patient-matched NP biopsy cores. For mRNA profiling, total RNA (1 μg) from each biopsy core was purified using the RNeasy Micro Kit (Qiagen) and interrogated with the Affymetrix Human Exon 1.0 ST GeneChip. For miRNA profiling, 250 ng of RNA from each biopsy core was isolated using the miRNeasy Kit (Qiagen,) and interrogated with the Agilent Human miRNA microarray V3 (Agilent Technologies). High-quality RNA samples were confirmed on the Agilent 2100 Bioanalyzer (Agilent Technologies). Affymetrix exon array data were normalized by quantile normalization with GC-RMA background correction, and data visualization and statistical analysis were performed by Partek Genomics

Published OnlineFirst June 18, 2015; DOI: 10.1158/1078-0432.CCR-14-1566

Suite 6.6 software (Partek) as previously described (13). Raw data from Agilent miRNA microarray analysis were quantile normalized and analyzed in GeneSpring GX program version 12.5 (Agilent Technologies). Identification of statistically significant, differentially expressed/regulated mRNAs and miRNAs was based on ANOVA or the paired *t* test with a 10% FDR criterion to correct for multiple testing (13). Microarray data can be assessed at GEO using accession numbers GSE64331 and GSE64318 for Affymetrix exon and Agilent miRNA arrays, respectively.

Principal component analysis (PCA) plots and hierarchical clustering of mRNA and miRNA data were performed using the Partek Genomics Suite 6.6. Two-dimensional (2D) hierarchical clustering analysis used average linkage and a Euclidean distance metric.

miRNA–miRNA pairings and pathway analysis

TargetScanHuman 6.2 was used to identify mRNAs predicted to be targets of the ANOVA-defined differentially expressed miRNAs. The list of predicted target mRNAs was intersected with the ANOVA-defined differentially expressed mRNAs to generate a catalog of experimental miRNA–mRNA pairings. Pairings were categorized as having reciprocal (e.g., miRNA up and mRNA down, or miRNA down and mRNA up), positive (i.e., miRNA up and mRNA up), or negative correlations (i.e., miRNA down and mRNA down) in AA prostate cancer vs. NP or AA prostate cancer vs. EA prostate cancer comparisons. The differentially expressed mRNAs not belonging to any pairings are herein referred to as unpaired mRNAs.

Global test (17) [and Gene Set Enrichment Analysis (GSEA; ref. 18) as a secondary confirmatory approach] was implemented to identify statistically significant canonical signaling pathways containing differentially regulated gene sets that may be associated with AA prostate cancer aggressiveness, based on AA prostate cancer versus AA NP, AA prostate cancer versus EA prostate cancer, and EA prostate cancer versus EA NP comparisons (detailed description in Supplementary Materials and Methods). Note that significant genes identified by the Global test and ANOVA may be mutually exclusive. Representative genes in different pathways identified by the Global test were chosen for validation if these genes were also identified by ANOVA and TargetScan prediction analyses as unpaired mRNAs or mRNAs belonging to miRNA–mRNA pairings. The underlying assumption was that genes fulfilling the above criteria would have a greater likelihood of validation success. Validation of differential gene expression was accomplished by quantitative RT-PCR (qRT-PCR) and immunohistochemistry (IHC) in cohorts of patient specimens separate from those used in microarray analysis (Supplementary Table S1B and S1C). Western analysis and functional assays in prostate cancer cell lines were performed to validate predicted reciprocal miRNA–mRNA pairings.

qRT-PCR validation of mRNAs and miRNAs

qRT-PCR validation was performed as previously described (19, 20). qRT-PCR determinations of mRNAs and miRNAs were performed in duplicate and normalized to levels of housekeeping genes *EIF1AX* and miR-103, respectively. *EIF1AX* and miR-103 are constitutively expressed and resistant to expression changes (19, 20). qRT-PCR primer pair sequences for mRNA and miRNA determinations are provided in Supplementary Tables S2 and S3, respectively. Sequences to entire mature miRNA are reported in miRBase database (21).

Tissue processing, IHC, and Western blot analysis

Serial sections of formalin-fixed, paraffin-embedded (FFPE) prostate cancer specimens from AA and EA patients with Gleason score 6 to 8 were immunolabeled. Western blot analysis, as previously described (13), was performed on AA and EA prostate cancer cell lines MDA PCa 2b, RC77T/E, VCaP, LNCaP, and PC-3. Details for tissue processing, IHC, image capturing/quantification, and cell line information can be found in Supplementary Materials and Methods.

Antibodies

Antibodies used in IHC assays and Western blotting analysis were rabbit monoclonal antibodies for STAT1 and pFOXO3A (Cell Signaling Technology), FOXO3A (Millipore), and AMACR (Dako), rabbit polyclonal antibody for MCL-1 (Santa Cruz Biotechnology), mouse monoclonal antibodies for p63 (Biocare Medical), and β-actin (Santa Cruz Biotechnology).

Functional analysis of prostate cancer cell lines following miRNA mimic or inhibitor transfections

Prostate cancer cells were transfected with either miRNA mimics or antagomirs using DharmaFECT4 transfection reagent (Dharmacon), according to the manufacturer's protocol. *MiR-133a* mimic, *miR-513c* mimic, *miR-96* mimic, *miR-34a* mimic, *miR-145* mimic, *miR-133a* antagomir, *miR-513c* antagomir, *miR-96* antagomir, and nonsense miRNA mimic and antagomir controls were purchased from Life Technologies.

In vitro functional assays, including cell proliferation, apoptosis, and invasion assays were conducted following miRNA mimic/antagomir transfections. Cell proliferation and apoptosis assays were performed using the BrdUrd Cell Proliferation Assay Kit (Calbiochem) and the Apo-ONE Caspase-3/7 Assay Kit (Promega) as described by the manufacturers. Detailed experimental design and protocols can be found in Supplementary Materials and Methods. Matrigel invasion assays were performed as previously described (19, 20).

Results

Microarray analysis reveals differentially expressed mRNAs and miRNAs in AA and EA prostate cancer patient specimens

In an earlier study (13), a total of 70 prostate biopsy cores (20 cancerous and 20 patient-matched NP from AA patients; 15 cancerous and 15 patient-matched NP from EA patients) were subjected to mRNA profiling, and a three-way comparison identified 2,908 significant (ANOVA, 10% FDR multiple test correction) differentially expressed mRNAs. In the present study, we have classified these mRNAs as follows, 433 mRNAs are "AA-enriched" (significantly overexpressed in AA) and 755 mRNAs are "AA-depleted" (significantly underexpressed in AA) based on the AA prostate cancer versus EA prostate cancer comparison (Supplementary Table S4). Another 980 mRNAs (up or down) are defined as "AA-specific" based on the AA prostate cancer versus AA NP comparison (and not significant in EA prostate cancer vs. EA NP), whereas 740 mRNAs are "EA-specific" based on EA prostate cancer versus EA NP (and not significant in AA prostate cancer vs. AA NP, Supplementary Table S4). PCA and 2D hierarchical clustering demonstrated clear separation and consistency of gene-expression profiles in the three separate comparisons (Fig. 1A).

Published OnlineFirst June 18, 2015; DOI: 10.1158/1078-0432.CCR-14-1566

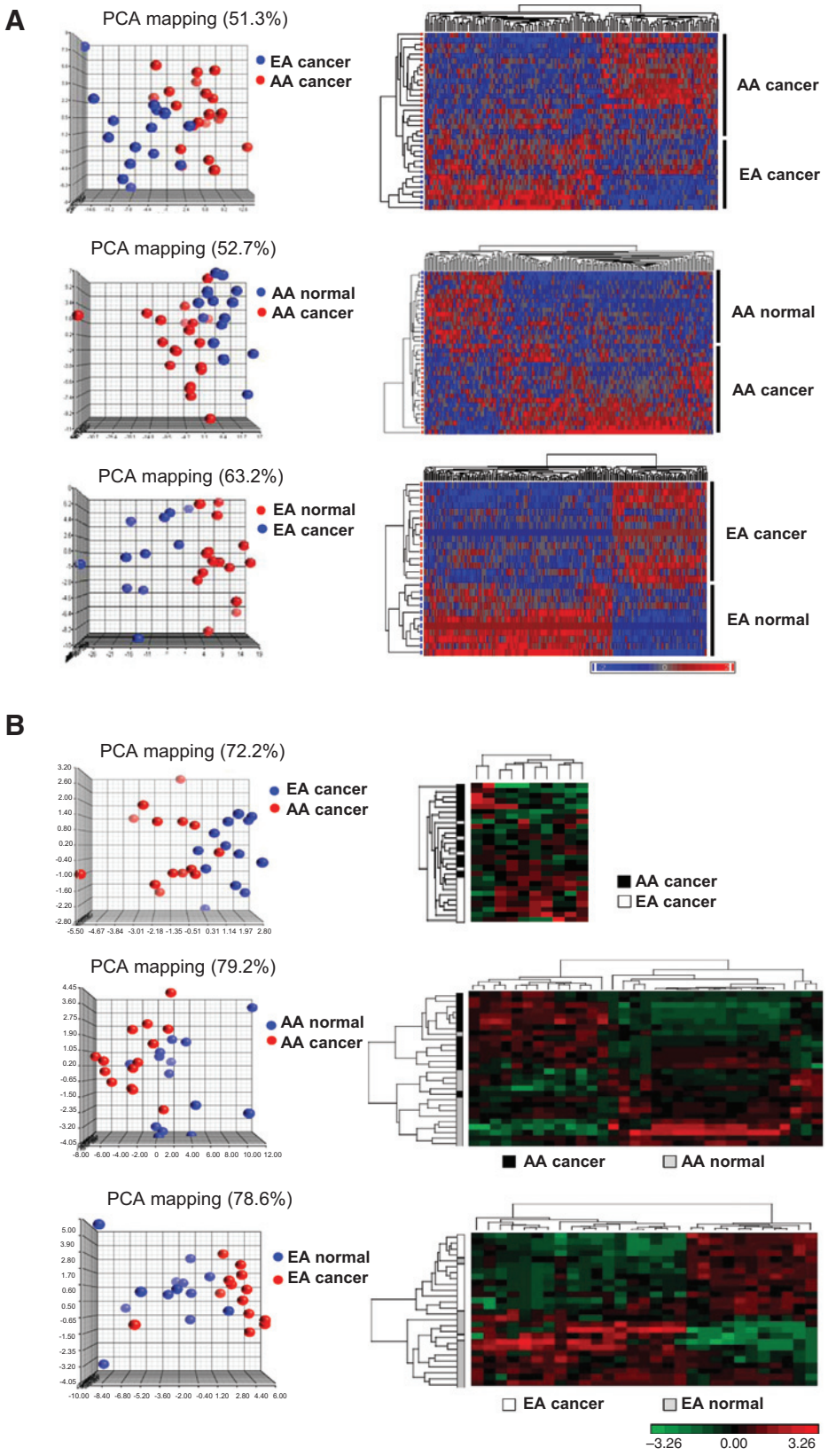

Figure 1.
mRNA and miRNA expression profiling of prostate cancer (PCa) specimens and patient-matched normal tissues derived from AA and EA patients. A, prostate cancer plots and hierarchical 2D clustering of mRNA expression in AA prostate cancer versus EA prostate cancer, and prostate cancer versus patient-matched normal tissue. B, prostate cancer plots and hierarchical clustergrams of miRNA expression in AA prostate cancer versus EA prostate cancer, and prostate cancer versus patient-matched normal tissue. For both A and B, samples are in rows, and mRNAs or miRNAs are in columns. Plots demonstrated clear separation and consistency of mRNA and miRNA expression profiles in group comparisons. For mRNA profiling, $n = 20$, 20, 15, and 15 for AA prostate cancer, AA-matched normal, EA prostate cancer, and EA-matched normal, respectively. For miRNA profiling, $n = 14$, 14, 13, and 13 for AA prostate cancer, AA-matched normal, EA prostate cancer, and EA-matched normal, respectively.

Published OnlineFirst June 18, 2015; DOI: 10.1158/1078-0432.CCR-14-1566

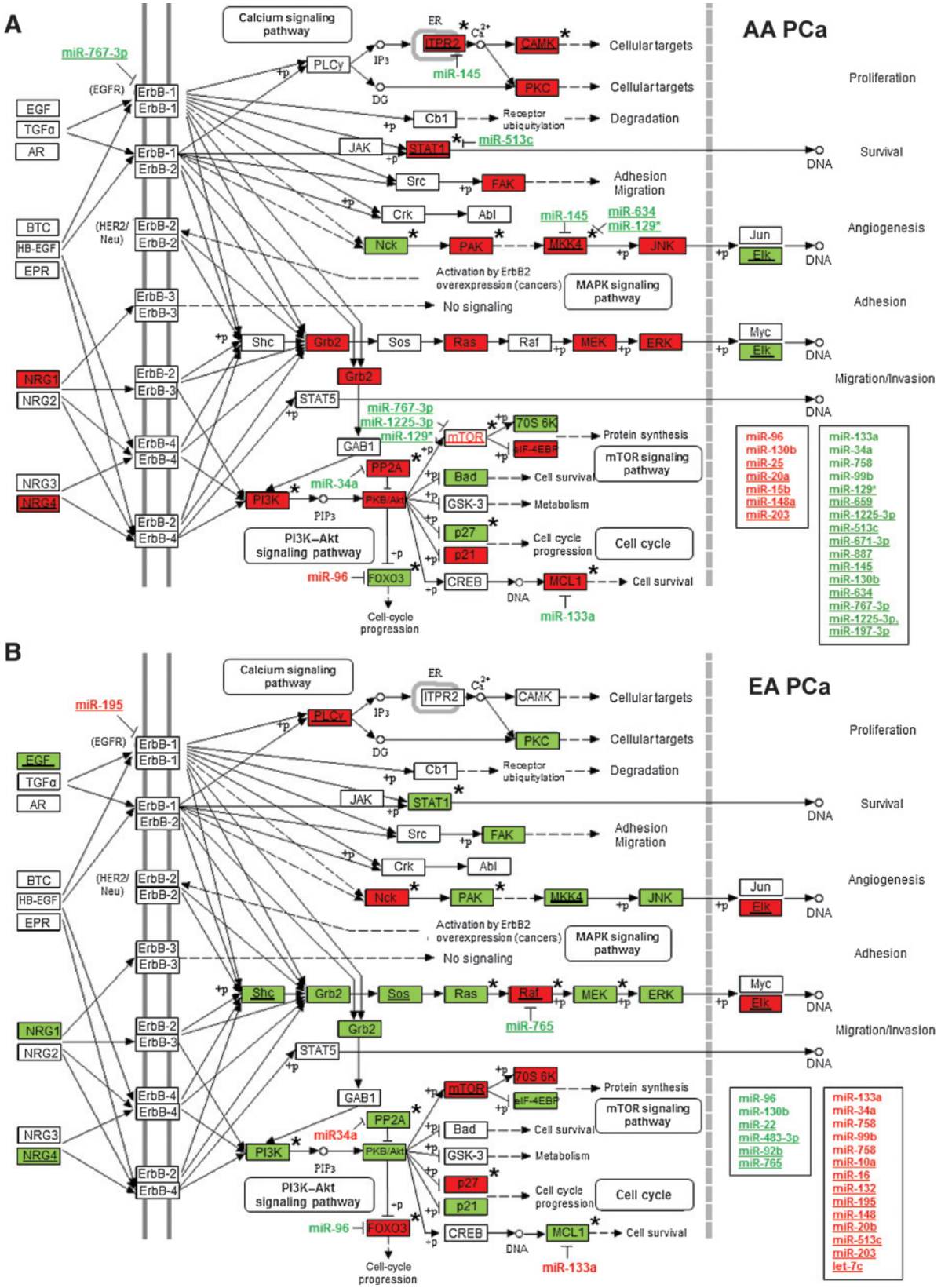

Published OnlineFirst June 18, 2015; DOI: 10.1158/1078-0432.CCR-14-1566

We also sought to investigate the relationship between miRNA and mRNA profiles in the same cohort of patients. Of the original 70 biopsy cores used for mRNA expression analysis, 54 provided sufficient material for miRNA expression profiling (14 cancerous and 14 patient-matched NP from AA patients; 13 cancerous and 13 patient-matched NP from EA patients). MiRNA profiling revealed 10, 33, and 29 miRNAs that were differentially expressed (ANOVA or paired *t* test, 10% FDR, fold change $\geq$ 1.5) between AA prostate cancer versus EA prostate cancer, AA prostate cancer versus AA NP and EA prostate cancer versus EA NP, respectively. Eleven of these miRNAs represent race-independent noncoding RNAs (miRNAs found significant in both AA prostate cancer vs. AA NP and EA prostate cancer vs. EA NP comparisons), along with 2 AA-enriched, 8 AA-depleted, 22 AA-specific and 18 EA-specific miRNAs (Supplementary Table S5). Prostate cancer and 2D hierarchical clustering demonstrated clear separation of miRNA profiles (Fig. 1B). In summary, we postulate that AA-enriched, AA-depleted, and race-specific miRNAs and mRNAs (but not race-independent mRNAs and miRNAs) may be associated with the biologic component of prostate cancer disparities.

Novel reciprocal miRNA–mRNA pairings and dysregulated-unpaired mRNAs in oncogenic signaling pathways promoting prostate cancer disparities

AA-enriched/-depleted, AA-specific and EA-specific miRNAs were analyzed by TargetScanHuman 6.2 (implemented in IPA miRNA Target Filter), resulting in the identification of 3,153, 5,244, and 3,812 predicted target mRNAs, respectively. We focused attention on those miRNA–mRNA pairings with the following criteria: (i) the predicted target mRNA was also differentially expressed in our microarray analysis (13), and (ii) the miRNA exhibited a reciprocal expression relationship with its target mRNA ("up–down" or "down–up"). Using these criteria, we have compiled 150 reciprocal miRNA–mRNA pairings in AA prostate cancer versus EA prostate cancer, 103 pairings in AA prostate cancer versus AA-matched NP and 137 pairings in EA prostate cancer versus EA-matched NP (Supplementary Table S6).

In a separate analysis to identify biologic pathways most significantly associated with AA prostate cancer aggressiveness, we applied the Global test to our gene-expression data from prostate biopsy cores. The Global test is a permutation-based approach, coupled with a penalized logistic regression model, to identify gene sets in pathways most significantly associated to clinical phenotypes/outcomes (17). Using this approach, we identified 124, 106, and 137 significant KEGG-annotated signaling pathways (FDR < 0.05) in AA prostate cancer versus EA prostate cancer, AA prostate cancer versus AA NP, and EA prostate cancer versus EA NP comparisons, respectively (Supplementary Table S7). Among the significant KEGG oncogenic pathways associated with AA prostate cancer were ERBB, MTOR, WNT, JAK-STAT, TGFβ, P53, and VEGF. Noteworthy was the ERBB pathway in AA prostate cancer, where a great majority of pathway genes (mRNAs) identified as significant by the Global test were upregulated in AA prostate cancer versus EA prostate cancer and AA prostate cancer versus AA NP comparisons (Fig. 2A; Supplementary Table S7). Conversely, the vast majority of significant genes in the ERBB pathway of EA prostate cancer were downregulated according to Global testing of EA prostate cancer versus AA prostate cancer and EA prostate cancer versus EA NP comparisons (Fig. 2B; Supplementary Table S7). Similar findings were obtained when analyzing our gene-expression data by the GSEA approach (Supplementary Table S8; ref. 18). Collectively, our pathway analysis suggests that differential gene regulation of ERBB signaling components in AA versus EA prostate cancer may play a critical role toward promoting prostate cancer disparities. A finding that may be particularly relevant given the well-developed targeted therapies for this critical oncogenic pathway (22, 23).

Next, we mapped the population-associated miRNAs and miRNA–mRNA pairings (Supplementary Tables S4, S5, and S6) onto the ERBB signaling pathway (Fig. 2). Altogether, 17 AA-specific miRNAs (miR-15b, miR-20a, miR-25, miR-148a, miR-203, miR-129*, miR-659, miR-125-3p, miR-513c, miR-671-3p, miR-887, miR-145, miR-130b, miR-634, miR-767-3p, miR-1225-3p, and miR-197-3p), 2 AA-enriched miRNAs (miR-96 and miR-130b) and 4 AA-depleted miRNAs (miR-133a, miR-758, miR-34a, and miR-99b) were predicted to target 56 of 85 signaling genes of the ERBB pathway in AA prostate cancer (Fig. 2A; Supplementary Table S6), leading to a projected overall activation of oncogenic signaling based on GO-Elite analysis (24). Of the reciprocal miRNA–mRNA pairings in the ERBB pathway of AA prostate cancer (Fig. 2A), 14 were novel (i.e., predicted miRNA targeting of mRNA not validated in literature), namely miR-133a/*MCL1* (down–up), miR-96/*PPP2R3A* (up–down), miR-133a/*PPP2R2D* (down–up), miR-767-3p/*MTOR* (down–up), miR-1225-3p/*MTOR* (down–up), miR-129*/*MTOR* (down–up), miR-129*/*PIK3AP1* (down–up), miR-96/*COL5A1* (up–down), miR-34a/*IKBKE* (down–up), miR-129*/*IKBKB* (down–up), mi-933/*IKBKB* (down–up), miR-145/*MKK4* (down–up), miR-634/*MKK4* (down–up), and miR-129*/*MKK4* (down–up; Supplementary Table S6).

In contrast with the projected activation of ERBB signaling in AA prostate cancer, EA prostate cancer was comprised mostly of downregulated oncogenes and upregulated EA-specific/-enriched miRNAs (predicted to target oncogenes) that were projected by GO-Elite to restrain ERBB pathway activity (Fig. 2B). Note that AA- and EA-specific miRNAs do not overlap by definition. Hence, the inverse expression pattern of AA- and EA-specific/enriched/

Figure 2.

The ERBB signaling pathway is highly activated in AA prostate cancer (PCa) specimens. Differentially expressed mRNAs [identified by Global test or Global test plus ANOVA (indicated by asterisk)] and miRNAs (identified by ANOVA or paired *t* test) populating the ERBB signaling pathway in AA prostate cancer (A) and EA prostate cancer (B). Upregulated (red) and downregulated (green) miRNAs with underline representing population-specific miRNAs, whereas miRNAs not underlined represent population-enriched (red) or -depleted (green) miRNAs. The same coloring and underlining scheme is used for differentially expressed mRNAs. The ERBB pathway in AA prostate cancer (A) is more highly activated compared with EA prostate cancer (B) as determined by GO-Elite. Eight novel reciprocal miRNA–mRNA pairings are highlighted, including miR-133a/*MCL1*, miR-96/*FOXO3A*, miR-513c/*STAT1*, miR-34a/*PPP2R2A*, miR-145/*ITPR2*, miR-145/*MKK4*, miR-634/*MKK4*, and miR-129*/*MKK4*. MiRNAs listed in boxes represent the population-specific (underlined) or -enriched/-depleted miRNAs predicted to target genes in the ERBB signaling pathway belonging to positively or negatively correlated pairings or nondifferentially expressed targets (see Supplementary Table S6).

Published OnlineFirst June 18, 2015; DOI: 10.1158/1078-0432.CCR-14-1566

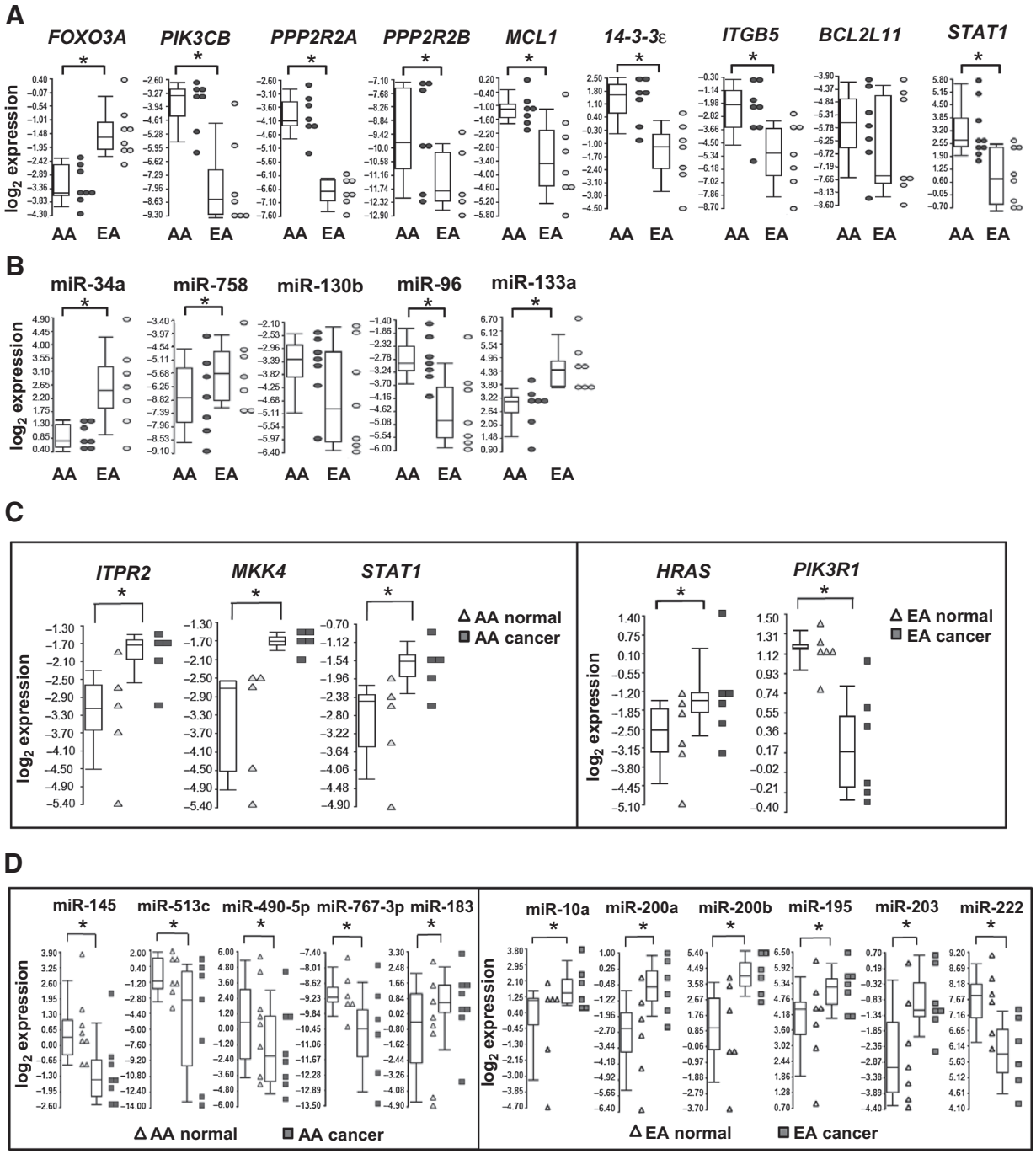

Figure 3.

qRT-PCR validation of population-enriched/-depleted and -specific mRNAs and miRNAs in AA and EA prostate cancer (PCa). A, qRT-PCR validation of differentially expressed mRNAs in AA prostate cancer versus EA prostate cancer. B, qRT-PCR validation of differentially expressed miRNAs in AA prostate cancer versus EA prostate cancer. C, qRT-PCR validation of population-specific mRNAs. D, qRT-PCR validation of population-specific miRNAs. The expression levels of mRNA or miRNAs from AA and EA patients are presented as Box-and-Whiskers plots (in A–D). Box: top quantile, median and bottom quantile. Whiskers: top extreme (90 percentile of the dataset) and bottom extreme (10 percentile of the dataset). Dot plots represent the relative expression levels of mRNA or miRNA from individual patient samples; *, $P < 0.05$ using the Student t test ($n = 6$–9 independent experiments in A and B), or a paired Student t test ($n = 5$–8 independent experiments in C and D).

depleted miRNAs targeting different components of the ERBB signaling pathway likely plays a critical role in the differential aggressiveness of prostate cancer progression in the two racial populations.

qRT-PCR validation in AA and EA prostate cancer biopsy specimens

qRT-PCR validation assays were performed in a second cohort of prostate cancer biopsy specimens from patients to validate our

Published OnlineFirst June 18, 2015; DOI: 10.1158/1078-0432.CCR-14-1566

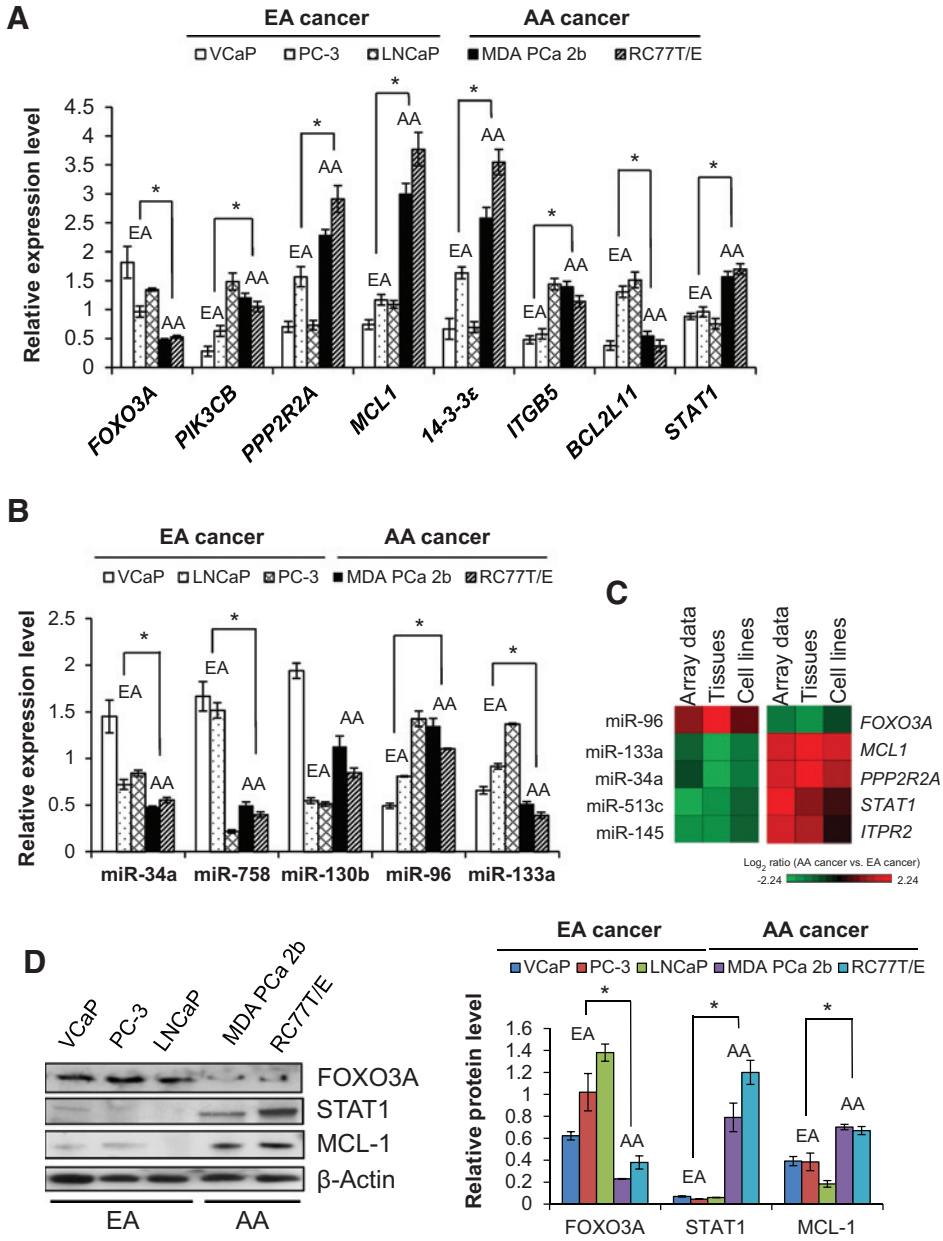

Figure 4.
Population-specific prostate cancer (PCa) cell lines are *in vitro* cell models for prostate cancer disparities. A, qRT-PCR validation of microarray mRNA data in population-specific prostate cancer cell lines. B, qRT-PCR validation of microarray miRNA data in population-specific prostate cancer cell lines. C, heat maps demonstrating inverse correlation between expression of miRNAs and mRNAs in AA prostate cancer versus EA prostate cancer comparisons. D, Western blot analysis reveals that protein expression correlates with mRNA expression in population-specific cell lines. Relative protein level was normalized to β-actin. Representative blots of 4 to 6 independent determinations. Data (in A, B, and D), mean ± SEM, with *, $P < 0.05$ using an unpaired Student *t* test, $n = 4$–6 independent experiments for each cell line. Means were derived by combining results from AA cell lines versus EA cell lines.

microarray analysis (Supplementary Table S1B). We specifically reassessed a combination of 30 differentially expressed miRNAs and mRNAs (identified as significant by both Global test and ANOVA; the exception being *BCL2L11* that was identified as significant by ANOVA only) residing in the ERBB signaling pathway, as well as four additional signaling pathways [i.e., non–small cell lung cancer (NSCLC) signaling, the JAK–STAT pathway, tight junction signaling, phosphatidylinositol signaling]. A comparison of the microarray and qRT-PCR results revealed high concordance (28 of 30) in our expression measurements. Successful validations included AA-enriched and -depleted mRNAs (Fig. 3A), AA-enriched and -depleted miRNAs (Fig. 3B), population-specific mRNAs (Fig. 3C) and population-specific miRNAs (Fig. 3D). Encompassed within the validations were the novel reciprocal miRNA–mRNA pairings miR-133a/*MCL1* (down–up; target mRNA significant in the ERBB pathway by the Global test), miR-96/*FOXO3A* (up–down; NSCLC signaling), miR-513c/*STAT1* (down–up; JAK–STAT pathway), miR-34a/*PPP2R2A* (down–up; tight junction signaling), miR-145/*ITPR2* (down–up; phosphatidylinositol signaling) and miR-145/*MKK4* (down–up; ERBB pathway; Figs. 2A and 3). Interestingly, four of the target mRNAs (*FOXO3A*, *STAT1*, *PPP2R2A*, and *ITPR2*) in these pairings are also known to participate downstream of ERBB signaling, and hence included in Fig. 2A for illustration (25–29).

qRT-PCR assessment of population-specific prostate cancer cell lines

We also assessed the expression of AA-enriched and -depleted miRNAs and mRNAs (depicted in Fig. 3) in a panel of prostate

Published OnlineFirst June 18, 2015; DOI: 10.1158/1078-0432.CCR-14-1566

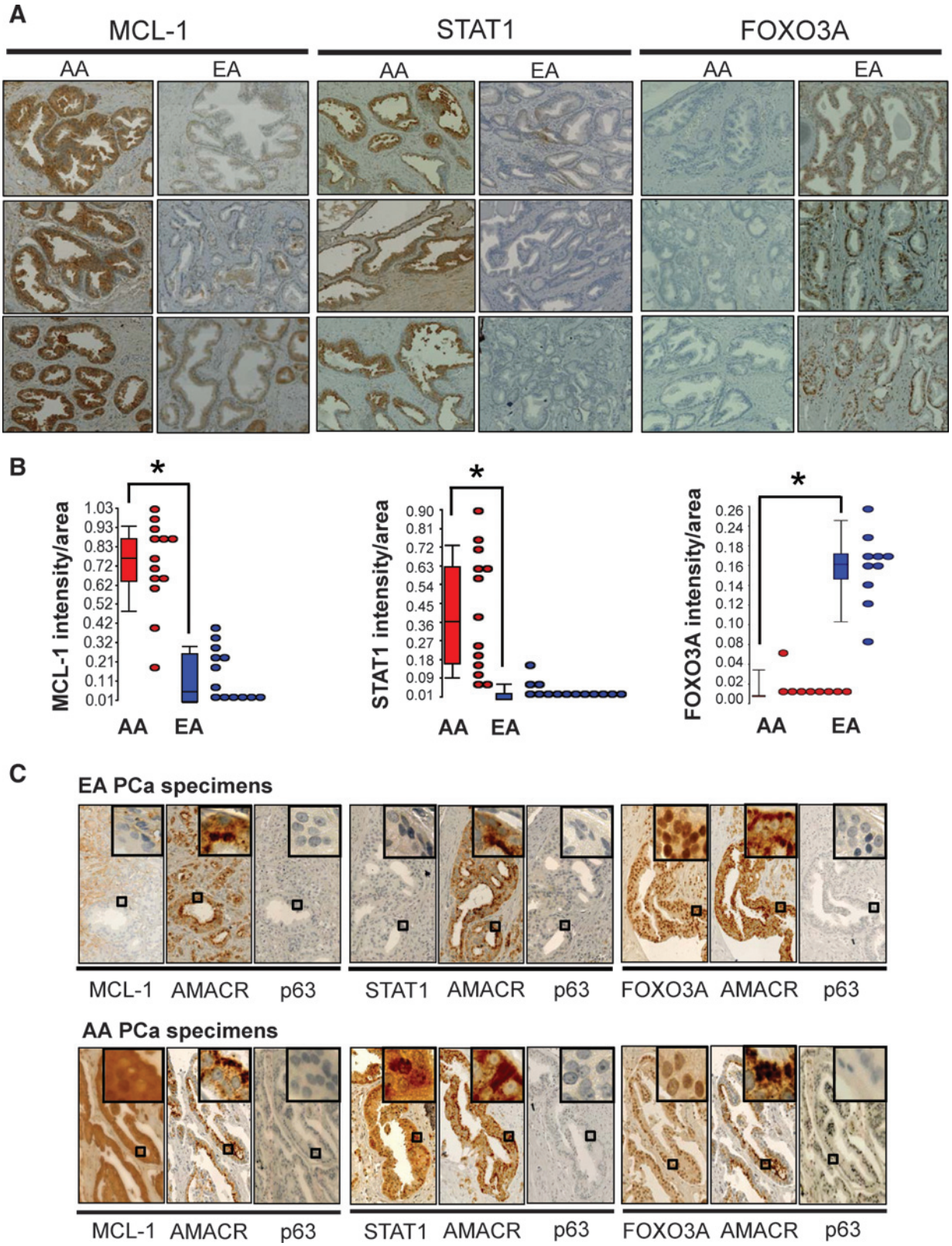

Published OnlineFirst June 18, 2015; DOI: 10.1158/1078-0432.CCR-14-1566

cancer cell lines derived from AA (MDA PCa 2b, RC77T/E) and EA patients (VCaP, LNCaP, and PC-3; see Supplementary Materials and Methods). There was strong overall agreement between the microarray data from patient specimens and qRT-PCR results of prostate cancer cell lines. Specifically, AA-depleted mRNAs (*FOXO3A* and *BCL2L11*) tended to be underexpressed in AA versus EA prostate cancer cell lines, and AA-enriched mRNAs (*PIK3CB*, *PPP2R2A*, *MCL1*, *14-3-3ε*, *ITGB5*, and *STAT1*) tended to be overexpressed in AA versus EA prostate cancer cell lines (Fig. 4A). An analogous consistency was observed for the miRNAs (Fig. 4B). Again, contained within these validations were the novel reciprocal miRNA–mRNA pairings miR-133a/*MCL1* (down–up), miR-96/*FOXO3A* (up–down), and miR-513c/*STAT1* (down–up; Fig. 4C). As a final consistency check, miRNA–mRNA pairings were found to be consistent with Western blot analysis where FOXO3A was underexpressed, whereas MCL-1 and STAT1 were overexpressed in AA versus EA prostate cancer cell lines (Fig. 4D).

Immunohistochemical assessment of MCL-1, STAT1, and FOXO3A in AA and EA prostate cancer specimens

Next, we examined protein expression of MCL-1, STAT1, and FOXO3A by immunohistochemical examination of archived FFPE prostate cancer specimens from AA and EA patients, representing a third cohort with associated Gleason scores ranging from 6 to 9 (Fig. 5A and B; Supplementary Table S1C and Fig. S1). To ensure that MCL-1, STAT1, and FOXO3A protein expression was indeed present in cancerous cells, another series of IHC was performed where our proteins of interest were examined along with alpha-methylacyl CoA racemase (AMACR; positive control for cancer cells) and p63 (marker for NP basal cells) in serial sections (30). IHC results demonstrated overexpression of MCL-1 and STAT1 in the cytoplasm of AA versus EA cancerous cells, and that the equivalent regions in adjacent sections stained strongly for AMACR but negative for p63 (Fig. 5B). For FOXO3A, staining was greater in the nuclei of EA versus AA cancerous cells, and in the equivalent regions of adjacent sections there was strong cytoplasmic staining for AMACR and negative staining for p63 in cancerous cells (Fig. 5B). In summary, our IHC findings in patient specimens perfectly match the Western results from prostate cancer cell lines.

Disruption of AA-specific and -enriched reciprocal miRNA–mRNA pairings affect cell proliferation, antiapoptosis, and invasion

To more firmly establish a causal link among our reciprocal miRNA–mRNA pairings, a series of miRNA mimics and antagomirs were transfected into population-specific prostate cancer cell lines and the protein products of predicted target mRNAs were measured by Western blot analysis. Two AA prostate cancer lines (RC77T/E, MDA PCa 2b) and 2 EA prostate cancer lines (LNCaP and PC-3) were chosen for *in vitro* functional assays on the basis of congruent qRT-PCR, Western and immunohistochemical findings (Figs. 4 and 5). Transfection of a *miR-133a* mimetic into AA and EA lines led to a downregulation of MCL-1 protein compared with cells transfected with nonsense control RNA (Fig. 6A, left). Conversely, *miR-133a* antagomir transfection into AA and EA lines led to an upregulation of MCL-1 protein compared with nonsense control (Fig. 6A, right). This antagomir-mediated upregulation in prostate cancer cells was anticipated given the "converse" mimetic-induced downregulation in prostate cancer cells. Analogous confirmatory findings were also demonstrated for AA-enriched miR-96 (predicted target *FOXO3A*) and downregulated AA-specific miR-513c (predicted target *STAT1*; Fig. 6A). Taken together, our *in vitro* mimic/antagomir manipulation of population-specific prostate cancer cell lines was consistent with observations in patient specimens (see Figs. 3 and 5), providing strong evidence of a causal link between our reciprocal miRNA–mRNA pairings.

The oncogenic consequences of disrupting steady-state expression of our prototype reciprocal pairings were assessed in AA lines RC77T/E and MDA PCa 2b, and EA lines LNCaP and PC-3. In the first set of functional assays, prostate cancer lines were transfected with a series of mimics, antagomirs, or nonsense control RNA and tested for proliferative activity using a bromodeoxyuridine (BrdUrd)-labeling assay. In each case, the *miR-133a* mimic, *miR-513c* mimic, and *miR-96* antagomir significantly suppressed proliferation of the AA and EA prostate cancer cell lines compared with nonsense control (Fig. 6B, top). Conversely, the majority of "converse" antagomir/mimic treatments (*miR-133a* antagomir, *miR-513c* antagomir, and *miR-96* mimic) significantly enhanced proliferation in both AA lines and EA line LNCaP, as anticipated (Fig. 6B, bottom). Interestingly, EA line PC-3 was completely resistant to the proliferation-inducing effects of all three "converse" antagomir/mimic treatments (Fig. 6B).

Next, apoptotic sensitivity in the absence and presence of 11 nmol/L docetaxel, a cytotoxic agent used in prostate cancer chemotherapy (31), was assessed in prostate cancer cell lines by caspase-3/7 activity assay. In the absence of any antagomir or mimic treatment, AA lines RC77T/E and MDA PCa 2b were chemoresistant to docetaxel-induced apoptosis (see nonsense control transfected cells in Fig. 6C, top). In contrast, docetaxel treatment alone significantly induced apoptosis in EA lines LNCaP and PC-3 (see nonsense control transfected cells in Fig. 6C, top). In the absence of docetaxel treatment, transfection of AA and EA cell lines with the *miR-133a* mimic, *miR-513c* mimic, or *miR-96* antagomir precipitated a generalized (exception being *miR-513c* mimic-transfected RC77T/E and LNCaP cells) and significant increase in apoptosis compared with nonsense control transfected cells (Fig. 6C, top). Strikingly in AA prostate cancer cells (but not in EA cells), the combination of a mimic or antagomir treatment with docetaxel

Figure 5.
IHC reveals differential protein expression in AA prostate cancer (PCa) versus EA prostate cancer. A, paraffin-embedded tissue sections of human prostate cancer specimens show strong MCL-1 and STAT1 expression in the cytoplasm of cancer cells of AA specimens, whereas FOXO3A immunoreactivity was detected in cancer cell nuclei of EA specimens. Images shown are representative of 13 AA and 13 EA specimens from different patients. B, the intensities of cytoplasmic MCL-1 and STAT1, and nuclear FOXO3A were quantified by using the ratio of total intensity of immunoreactive MCL-1, STAT1, or FOXO3A over the total area of cells in the images. Data, box plots of $n = 13$ AA or EA samples, with *, $P < 0.05$ using the Student t test. C, serial FFPE sections derived from AA and EA prostate cancer patients were immunostained for AMACR (a prostate cancer marker), p63 (a normal basal cell marker) and the protein of interest (MCL-1, STAT1, or FOXO3A). Enlarged pictures (rectangles as indicated) enhance the nuclear or cytoplasmic distribution of these proteins at the cellular level.

Published OnlineFirst June 18, 2015; DOI: 10.1158/1078-0432.CCR-14-1566

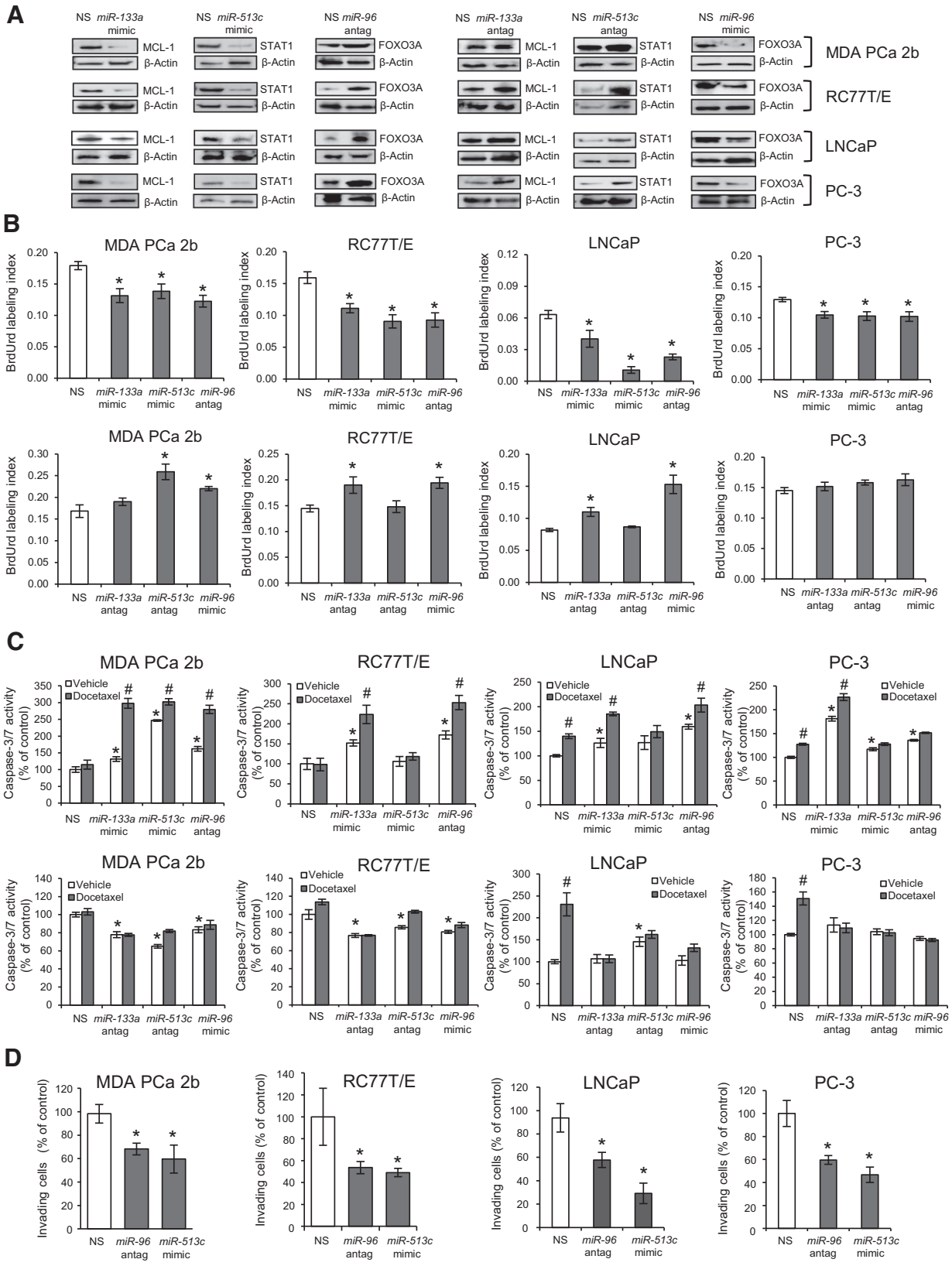

Published OnlineFirst June 18, 2015; DOI: 10.1158/1078-0432.CCR-14-1566

treatment resulted in apoptotic activity that was greater than either treatment alone, suggesting that disruption of key miRNAs sensitized cells to docetaxel (Fig. 6C, top). Interestingly, the "converse" antagomir/mimic treatments (*miR-133a* antagomir, *miR-513c* antagomir, and *miR-96* mimic) in the absence of docetaxel had the effect of rendering AA lines, but not EA lines, more resistant to apoptosis (Fig. 6C, bottom). On the basis of the proliferative and apoptotic findings, EA prostate cancer lines compared with AA lines appear to be less susceptible to the oncogenic-promoting effects of the reciprocal pairs miR-133a/*MCL1*, miR-96/*FOXO3A*, and miR-513c/*STAT1*.

Finally, the consequences of disrupting steady-state expression of our prototype reciprocal pairings on the invasive activity of prostate cancer cell lines were assessed by Matrigel assay. Both *miR-513c* mimic and *miR-96* antagomir treatments in AA lines RC77T/E and MDA PCa 2b, and EA lines LNCaP and PC-3 resulted in a significant decrease in invasive activity (Fig. 6D), though we cannot discount the possibility that this decrease may be due in part to decreased proliferative activity (Fig. 6B, top). In an attempt to identify reciprocal pairings that modulate invasion without affecting proliferation, we tested two additional down–up pairings (miR-145/*ITPR2* and miR-34a/*PPP2R2A* in the EGFR–PI3K–AKT pathway) in the AA prostate cancer lines. Western blot analysis confirmed a causal link for these two reciprocal pairings, as transfection with either the *miR-145* mimic or *miR-34a* mimic in AA lines resulted in a reduction of ITPR2 or PPP2R2A protein levels, respectively (Supplementary Fig. S2A). As shown in Supplementary Fig. S2B, the *miR-145* mimic affected both proliferation and invasion, whereas the *miR-34a* mimic was associated with a significant decrease in invasion and had no effect on proliferation in both AA prostate cancer cell lines. Taken together, these findings support the notion that depletion of miR-133a (leading to upregulation of MCL1), miR-513c (upregulation of STAT1), miR145 (upregulation of ITPR2), and miR-34a (upregulation of PPP2R2A), coupled with enrichment of miR-96 (downregulation of FOXO3A) collectively drives proliferation, chemoresistance and/or invasion in AA prostate cancer cells.

Discussion

In this study, we performed an integrated analysis of differential miRNA and mRNA expression profiles in prostate cancer and NP specimens derived from AA and EA patients. Our goal was to identify significant oncogenic signaling pathways that are populated with AA-specific/-enriched reciprocal miRNA–mRNA pairs. Emphasis was placed on cataloging novel reciprocal pairs (i.e., predicted miRNA targeting of the mRNA has yet to be experimentally validated). The underlying hypothesis being that these novel reciprocal pairs may play a mechanistic role in prostate cancer disparities (i.e., more aggressive nature of AA prostate cancer), which could be assessed by systematically disrupting reciprocal pairs with mimic/antagomir treatment of population-specific prostate cancer cell lines and testing for a loss (or gain) of oncogenic function. To date, the integrated analysis of miRNA–mRNA pairs has been limited to a handful of prostate cancer studies (32, 33) and none have been related to prostate cancer disparities.

There are a number of available miRNA-target mRNA prediction algorithms (34). However, it is estimated that up to 40% of all miRNA-target mRNA predictions are false positives (35), representing a major obstacle in the identification of true miRNA–mRNA interacting partnerships with functional consequences in cancer. An approach exploited by this study was to incorporate both a sequence-based algorithm for miRNA target predictions and focusing on miRNA–mRNA predictions exhibiting reciprocal differential expression profiles (up–down and down–up). Such a strategy has been demonstrated to provide more accurate predictions (35). A total of 390 reciprocal pairings were identified in prostate cancer and NP specimens from AA and EA patients. These pairs (along with unpaired differentially expressed miRNAs and mRNAs) were found populated in 19 and 18 significant cancer signaling pathways from the perspective of AA and EA prostate cancer, respectively.

ERBB signaling pathway in prostate cancer disparities

The ERBB signaling pathway is regarded as a critical oncogenic signaling pathway in cancer, as mutations and/or overexpression of the EGFR and mutations in multiple PI3K isoforms are frequently detected in various types of cancers, including prostate, head and neck, renal, lung, breast, colon, ovarian, glioma, pancreas, and bladder cancers (22, 23). In terms of prostate cancer disparities, EGFR overexpression has been shown to be significantly associated with AA patients (11). Our findings suggest that 18 reciprocal miRNA–mRNA pairs populating the EGFR–PI3K–AKT signaling pathway in AA prostate cancer, and likely working in concert with overexpressed EGFR (11), drive AA prostate cancer.

MiR-513c/*STAT1* (down–up) represented a novel predicted pairing, and miR-513c has previously been shown to be downregulated in neuroendocrine lung tumors (36). However, the role of miR-513c in cancer and the identification of its target mRNA(s) have remained undetermined. Our results demonstrate for the first time that *STAT1* serves as a target of miR-513c. The STAT1

Figure 6.
Functional validation of miR-133a/*MCL1*, miR-513c/*STAT1*, and miR-96/*FOXO3A* pairs in prostate cancer (PCa) aggressiveness. A, overexpression of *miR-133a* mimic, *miR-513c* mimic, or *miR-96* antagomir in prostate cancer cell lines resulted in downregulation of MCL-1 and STAT1, and upregulation of FOXO3A, respectively. In contrast, inhibition of *miR-133a* or *miR-513c* with antagomirs or overexpression of *miR-96* mimic resulted in upregulation of MCL-1 and STAT1, and downregulation of FOXO3A. AA lines are MDA PCa 2B, RC77T/E, and EA cell lines are LNCaP and PC-3. Representative Western blots from three to six independent experiments. B, BrdUrd-labeled cell proliferation assays of prostate cancer cell lines transfected with *miR-133a* mimic, *miR-513c* mimic or *miR-96* antagomir, or "converse" antagomir/mimic treatments (*miR-133a* antagomir, *miR-513c* antagomir, or *miR-96* mimic) were compared with cells treated with NS (nonsense scrambled negative control). Data, mean ± SEM of $n = 3$–4 independent experiments, with *, $P < 0.05$ using ANOVA and Tukey *post hoc* test. C, apoptosis assays in population-specific prostate cancer cell lines transfected with mimics or antagomirs. Apoptosis activity was assayed by measuring caspase-3/7 activity using the Apo-ONE Kit (Promega), and the data were normalized to caspase-3/7 level of vehicle-treated NS control. Data, mean ± SEM for $n = 3$–6 independent experiments, with $P < 0.05$ using ANOVA and Tukey *post hoc* test comparing mimic or antagomir transfection plus vehicle treatment to NS transfection plus vehicle (*), or mimic or antagomir transfection plus vehicle to mimic or antagomir transfection plus docetaxel (#). D, prostate cancer cells transfected with *miR-96* antagomir or *miR-513c* mimic were significantly less invasive compared with NS control-treated cells. Data, mean ± SEM of $n = 4$–6 independent experiments, with *, $P < 0.05$ using ANOVA and Holmes *post hoc* test; Antag, antagomir.

Published OnlineFirst June 18, 2015; DOI: 10.1158/1078-0432.CCR-14-1566

protein is a transcription factor and its overexpression in prostate cancer cells has been associated with docetaxel resistance (37). Interestingly, the AA prostate cancer cell lines investigated in this study were resistant to docetaxel-induced apoptosis, but became sensitized upon treatment with a *miR-513c* mimic that downregulated STAT1. Additional functions of the miR-513c/*STAT1* pair in AA prostate cancer cells include proliferation and invasion, as disruption of this pairing with a *miR-513c* mimic resulted in a loss of proliferative and invasive activities. The role of miR-513c/*STAT1* in driving AA prostate cancer was further supported by experiments using a "converse" targeting approach (i.e., *miR-513c* antagomir) in EA prostate cancer cell lines, resulting in STAT1 upregulation and a more aggressive phenotype reminiscent of the AA prostate cancer lines (i.e., increased proliferation and chemoresistance).

Downregulation of *miR-133a* has been observed in various cancers (38), acting as a tumor suppressor by targeting multiple oncogenes, such as *FSCN1*, *MMP14*, *LASP1*, *EGFR*, *IGF1R*, and *GSTP1* (39). In our study, *MCL1* was identified as a novel target of miR-133a, and overexpression of a *miR-133a* mimic in prostate cancer cell lines led to a downregulation of MCL-1 protein and a corresponding decrease in proliferative activity, as well as loss of chemoresistance to docetaxel. MCL-1 has been demonstrated to be overexpressed in prostate cancer and is linked to higher Gleason scores and increased bone metastasis in prostate cancer patients (29). As was the case for miR-513c/*STAT1*, we demonstrated a role of miR-133a/*MCL1* in driving AA prostate cancer by using a "converse" targeting approach (i.e., *miR-133a* antagomir) in EA prostate cancer cell lines, resulting in MCL-1 upregulation and a more aggressive phenotype, again reminiscent of the AA prostate cancer lines.

Upregulation of miR-96 has been observed in lung, breast, bladder, and colorectal cancers (40). MiR-96 promotes cell proliferation by targeting the *FOXO1* gene, encoding a transcription factor, in breast and prostate cancer (41, 42); and enhances proliferative, invasive, and migratory activity by targeting *FOXO1* and *RECK* in breast cancer, bladder, and lung cancers (43, 44). In this study, we further demonstrated that *FOXO3A* targeted by miR-96 in prostate cancer, confirming a previous observation in breast cancer (45). Disruption of miR-96/*FOXO3A* (up–down) in AA prostate cancer cell lines with a *miR-96* antagomir resulted in FOXO3A protein upregulation and a corresponding decrease in proliferative, invasive, and chemoresistant activities. Conversely, introduction of a *miR-96* mimic into EA prostate cancer cell lines had the opposite effect by downregulating FOXO3A protein and promoting proliferation and chemoresistance. In essence, the EA prostate cancer cell lines transformed into a more aggressive AA prostate cancer–like phenotype. Taken together, these findings are consistent with the known tumor-suppressor effect of FOXO3A in prostate cancer (46).

Another intriguing miRNA–mRNA pair residing in the ERBB signaling pathway of AA prostate cancer is miR-145/*ITPR2* (down–up). Recent genome-wide association studies have implicated the inositol 1,4,5-triphosphate receptor type 2 (*ITPR2*) gene as a novel risk locus for renal cell carcinoma (47, 48). MiR-145 has been implicated as a tumor-suppressive miRNA as it is downregulated in different cancers and its expression has been associated with an inhibition of prostate cancer cell invasion and migration *in vitro* (49). Our findings link miR-145 and *ITPR2* for the first time as a functional reciprocal pair that promotes invasion and proliferation in AA prostate cancer.

It should also be noted that AA prostate cancer was associated with a large number of upregulated oncogenes (such as *ITGA5*, *PIK3CB*, *PIK3AP*, *ITPR2*, *STAT1*, *CSNK2A1*, *MKK4*, *14-3-3ε*, *MTOR*, and *MCL1*) as well as dysregulated unpaired miRNAs that are unique to AA prostate cancer (e.g., AA-specific/depleted miRNAs) and computationally predicted to target EGFR–PI3K–AKT signaling components (such as *EGFR*, *AKT3*, *GSK3*, *JAK1*, *JUN*, and *KRAS*) leading to pathway activation. Conversely, our analysis identified an equally large number of dysregulated oncogenes plus unpaired miRNAs that were specific to EA prostate cancer and computationally predicted to target a different set of EGFR–PI3K–AKT signaling components leading to pathway suppression. Also noteworthy, unpaired AA-specific miR-767-3p (downregulated in AA prostate cancer vs. AA NP) and unpaired EA-specific miR-195 (upregulated in EA prostate cancer vs. EA NP) were both predicted to target the *EGFR* mRNA, resulting in an anticipated up- and downregulation of the EGFR protein, respectively. This finding would be consistent with the observed racial disparity of EGFR overexpression in AA prostate cancer (11). Although our analysis has focused on five reciprocal miRNA–mRNA pairings, it is important to stress that the miRNAs in these pairings would be expected to coordinately target other mRNAs (i.e., *MCL1*, *FSCN1*, *MMP14*, *LASP1*, *EGFR*, *IGF1R* and *GSTP1* by miR-133a, and *FOXO3A*, *FOXO1* and *RECK* by miR-96), presumably leading to the aggressive phenotypic features found in AA prostate cancer. Finally, our findings suggest that these deregulated miRNA–mRNA pairs, uniquely found in AA prostate cancer, appear to target the EGFR–PI3K–AKT axis, thus driving prostate cancer aggressiveness in the AA population.

Understanding the origins and etiology of cancer disparities is a complex endeavor and it is imperative that such disparities be addressed at all levels of intervention, both social and biologic. Evidence exists, indicating that one component of the disparity may be related to biologic differences in the molecular etiology of the disease resulting in tumor aggressiveness. We have used a population-based comparative approach in an attempt to discern potential drivers of prostate cancer aggressiveness and have identified novel pathway alterations in miRNA–mRNA pairs that may contribute to prostate cancer disparities. Given the projected use of miRNA mimics and antagomirs as potential cancer therapeutics (50), our study serves as a first pass catalog of dysregulated miRNA–mRNA pairs residing in key oncogenic signaling pathways in AA prostate cancer.

Disclosure of Potential Conflicts of Interest

No potential conflicts of interest were disclosed.

Authors' Contributions

Conception and design: B.-D. Wang, Y. Ji, J. Rhim, S.R. Patierno, N.H. Lee
Development of methodology: B.-D. Wang, V. Patel, A. Popratiloff, P. Latham, N.H. Lee
Acquisition of data (provided animals, acquired and managed patients, provided facilities, etc.): B.-D. Wang, K. Ceniccola, Q. Yang, R. Andrawis, A. Popratiloff, P. Latham, N.H. Lee
Analysis and interpretation of data (e.g., statistical analysis, biostatistics, computational analysis): B.-D. Wang, K. Ceniccola, J. Olender, A. Popratiloff, P. Latham, Y. Lai, N.H. Lee
Writing, review, and/or revision of the manuscript: B.-D. Wang, K. Ceniccola, Y. Ji, J. Rhim, J. Olender, A. Popratiloff, P. Latham, N.H. Lee
Administrative, technical, or material support (i.e., reporting or organizing data, constructing databases): B.-D. Wang, R. Andrawis, J. Olender, N.H. Lee
Study supervision: S.R. Patierno, N.H. Lee

Published OnlineFirst June 18, 2015; DOI: 10.1158/1078-0432.CCR-14-1566

Grant Support

This work was supported by NCI grant R01 CA120316 (to N.H. Lee), DOD grant PC121975 (to N.H. Lee), Affymetrix Collaborations in Cancer Research Award (to N.H. Lee), NCI supplement grant U01 CA116937 (to S.R. Patierno), and American Cancer Society grant IRG-08-091-01 (to B.-D. Wang).

The costs of publication of this article were defrayed in part by the payment of page charges. This article must therefore be hereby marked *advertisement* in accordance with 18 U.S.C. Section 1734 solely to indicate this fact.

Received June 22, 2014; revised April 30, 2015; accepted June 8, 2015; published OnlineFirst June 18, 2015.

References

1. Volinia S, Calin GA, Liu CG, Ambs S, Cimmino A, Petrocca F, et al. A microRNA expression signature of human solid tumors defines cancer gene targets. Proc Natl Acad Sci U S A 2006;103:2257–61.
2. Esquela-Kerscher A, Slack FJ. Oncomirs - microRNAs with a role in cancer. Nat Rev Cancer 2006;6:259–69.
3. Cummins JM, Velculescu VE. Implications of micro-RNA profiling for cancer diagnosis. Oncogene 2006;25:6220–7.
4. Calin GA, Liu CG, Sevignani C, Ferracin M, Felli N, Dumitru CD, et al. MicroRNA profiling reveals distinct signatures in B cell chronic lymphocytic leukemias. Proc Natl Acad Sci U S A 2004;101:11755–60.
5. Lee YS, Dutta A. MicroRNAs in cancer. Annu Rev Pathol 2009;4:199–227.
6. Shi XB, Tepper CG, White RW. MicroRNAs and prostate cancer. J Cell Mol Med 2008;12:1456–65.
7. Jemal A, Siegel R, Ward E, Murray T, Xu J, Thun MJ. Cancer statistics, 2007. CA Cancer J Clin 2007;57:43–66.
8. Powell IJ. Epidemiology and pathophysiology of prostate cancer in African-American men. J Urol 2007;177:444–9.
9. Evans S, Metcalfe C, Ibrahim F, Persad R, Ben-Shlomo Y. Investigating Black-White differences in prostate cancer prognosis: a systematic review and meta-analysis. Int J Cancer 2008;123:430–5.
10. Devgan SA, Henderson BE, Yu MC, Shi CY, Pike MC, Ross RK, et al. Genetic variation of 3 beta-hydroxysteroid dehydrogenase type II in three racial/ethnic groups: implications for prostate cancer risk. Prostate 1997;33:9–12.
11. Shuch B, Mikhail M, Satagopan J, Lee P, Yee H, Chang C, et al. Racial disparity of epidermal growth factor receptor expression in prostate cancer. J Clin Oncol 2004;22:4725–9.
12. Wallace TA, Prueitt RL, Yi M, Howe TM, Gillespie JW, Yfantis HG, et al. Tumor immunobiological differences in prostate cancer between African-American and European-American men. Cancer Res 2008;68:927–36.
13. Wang BD, Yang Q, Ceniccola K, Bianco F, Andrawis R, Jarrett T, et al. Androgen receptor-target genes in African American prostate cancer disparities. Prostate Cancer 2013;2013:763569.
14. Ozen M, Creighton CJ, Ozdemir M, Ittmann M. Widespread deregulation of microRNA expression in human prostate cancer. Oncogene 2008;27:1788–93.
15. Wang L, Tang H, Thayanithy V, Subramanian S, Oberg AL, Cunningham JM, et al. Gene networks and microRNAs implicated in aggressive prostate cancer. Cancer Res 2009;69:9490–7.
16. Pomerantz MM, Beckwith CA, Regan MM, Wyman SK, Petrovics G, Chen Y, et al. Evaluation of the 8q24 prostate cancer risk locus and MYC expression. Cancer Res 2009;69:5568–74.
17. Goeman JJ, van de Geer SA, de Kort F, van Houwelingen HC. A global test for groups of genes: testing association with a clinical outcome. Bioinformatics 2004;20:93–9.
18. Tian L, Greenberg SA, Kong SW, Altschuler J, Kohane IS, Park PJ. Discovering statistically significant pathways in expression profiling studies. Proc Natl Acad Sci U S A 2005;102:13544–9.
19. House CD, Vaske CJ, Schwartz AM, Obias V, Frank B, Luu T, et al. Voltage-gated Na+ channel SCN5A is a key regulator of a gene transcriptional network that controls colon cancer invasion. Cancer Res 2010;70:6957–67.
20. Wang BD, Kline CL, Pastor DM, Olson TL, Frank B, Luu T, et al. Prostate apoptosis response protein 4 sensitizes human colon cancer cells to chemotherapeutic 5-FU through mediation of an NF kappaB and microRNA network. Mol Cancer 2010;9:98.
21. Griffiths-Jones S, Saini HK, van Dongen S, Enright AJ. miRBase: tools for microRNA genomics. Nucleic Acids Res 2008;36:D154–8.
22. Wong KK, Engelman JA, Cantley LC. Targeting the PI3K signaling pathway in cancer. Curr Opin Genet Dev 2010;20:87–90.
23. Seshacharyulu P, Ponnusamy MP, Haridas D, Jain M, Ganti AK, Batra SK. Targeting the EGFR signaling pathway in cancer therapy. Expert Opin Ther Targets 2012;16:15–31.
24. Zambon AC, Gaj S, Ho I, Hanspers K, Vranizan K, Evelo CT, et al. GO-Elite: a flexible solution for pathway and ontology over-representation. Bioinformatics 2012;28:2209–10.
25. Zhu G, Fan Z, Ding M, Zhang H, Mu L, Ding Y, et al. An EGFR/PI3K/AKT axis promotes accumulation of the Rac1-GEF Tiam1 that is critical in EGFR-driven tumorigenesis. Oncogene. 2015 Mar 9. [Epub ahead of print].
26. Han W, Carpenter RL, Cao X, Lo HW. STAT1 gene expression is enhanced by nuclear EGFR and HER2 via cooperation with STAT3. Mol Carcinog 2013;52:959–69.
27. Cronshaw DG, Kouroumalis A, Parry R, Webb A, Brown Z, Ward SG. Evidence that phospholipase-C-dependent, calcium-independent mechanisms are required for directional migration of T-lymphocytes in response to the CCR4 ligands CCL17 and CCL22. J Leukoc Biol 2006;79:1369–80.
28. Krol J, Francis RE, Albergaria A, Sunters A, Polychronis A, Coombes RC, et al. The transcription factor FOXO3a is a crucial cellular target of gefitinib (Iressa) in breast cancer cells. Mol Cancer Ther 2007;6:3169–79.
29. Zhang S, Zhau HE, Osunkoya AO, Iqbal S, Yang X, Fan S, et al. Vascular endothelial growth factor regulates myeloid cell leukemia-1 expression through neuropilin-1-dependent activation of c-MET signaling in human prostate cancer cells. Mol Cancer 2010;9:9.
30. Signoretti S, Waltregny D, Dilks J, Isaac B, Lin D, Garraway L, et al. p63 is a prostate basal cell marker and is required for prostate development. Am J Pathol 2000;157:1769–75.
31. Tannock IF, de Wit R, Berry WR, Horti J, Pluzanska A, Chi KN, et al. Docetaxel plus prednisone or mitoxantrone plus prednisone for advanced prostate cancer. N Engl J Med 2004;351:1502–12.
32. Gade S, Porzelius C, Falth M, Brase JC, Wuttig D, Kuner R, et al. Graph based fusion of miRNA and mRNA expression data improves clinical outcome prediction in prostate cancer. BMC Bioinformatics 2011;12:488.
33. Feng J, Huang C, Diao X, Fan M, Wang P, Xiao Y, et al. Screening biomarkers of prostate cancer by integrating microRNA and mRNA microarrays. Genet Test Mol Biomarkers 2013;17:807–13.
34. Zheng H, Fu R, Wang JT, Liu Q, Chen H, Jiang SW. Advances in the techniques for the prediction of microRNA targets. Int J Mol Sci 2013;14:8179–87.
35. Huang JC, Babak T, Corson TW, Chua G, Khan S, Gallie BL, et al. Using expression profiling data to identify human microRNA targets. Nat Methods 2007;4:1045–9.
36. Mairinger FD, Ting S, Werner R, Walter RF, Hager T, Vollbrecht C, et al. Different micro-RNA expression profiles distinguish subtypes of neuroendocrine tumors of the lung: results of a profiling study. Mod Pathol 2014;27:1632–40.
37. Patterson SG, Wei S, Chen X, Sallman DA, Gilvary DL, Zhong B, et al. Novel role of Stat1 in the development of docetaxel resistance in prostate tumor cells. Oncogene 2006;25:6113–22.
38. Nohata N, Hanazawa T, Enokida H, Seki N. microRNA-1/133a and microRNA-206/133b clusters: dysregulation and functional roles in human cancers. Oncotarget 2012;3:9–21.
39. Uchida Y, Chiyomaru T, Enokida H, Kawakami K, Tatarano S, Kawahara K, et al. MiR-133a induces apoptosis through direct regulation of GSTP1 in bladder cancer cell lines. Urol Oncol 2013;31:115–23.
40. Xu XM, Qian JC, Deng ZL, Cai Z, Tang T, Wang P, et al. Expression of miR-21, miR-31, miR-96 and miR-135b is correlated with the clinical parameters of colorectal cancer. Oncol Lett 2012;4:339–45.
41. Guttilla IK, White BA. Coordinate regulation of FOXO1 by miR-27a, miR-96, and miR-182 in breast cancer cells. J Biol Chem 2009;284:23204–16.
42. Haflidadottir BS, Larne O, Martin M, Persson M, Edsjo A, Bjartell A, et al. Upregulation of miR-96 enhances cellular proliferation of prostate cancer cells through FOXO1. PLoS ONE 2013;8:e72400.

Published OnlineFirst June 18, 2015; DOI: 10.1158/1078-0432.CCR-14-1566

43. Guo H, Li Q, Li W, Zheng T, Zhao S, Liu Z. miR-96 downregulates RECK to promote growth and motility of non–small cell lung cancer cells. Mol Cell Biochem 2014;390:155–60.
44. Zhang J, Kong X, Li J, Luo Q, Li X, Shen L, et al. miR-96 promotes tumor proliferation and invasion by targeting RECK in breast cancer. Oncol Rep 2014;31:1357–63.
45. Lin H, Dai T, Xiong H, Zhao X, Chen X, Yu C, et al. Unregulated miR-96 induces cell proliferation in human breast cancer by downregulating transcriptional factor FOXO3a. PLoS ONE 2010;5:e15797.
46. Shukla S, Bhaskaran N, Maclennan GT, Gupta S. Deregulation of FoxO3a accelerates prostate cancer progression in TRAMP mice. Prostate 2013;73:1507–17.
47. Audenet F, Cancel-Tassin G, Bigot P, Audouin M, Gaffory C, Ondet V, et al. Germline genetic variations at 11q13 and 12p11 locus modulate age at onset for renal cell carcinoma. J Urol 2014;191:487–92.
48. Wu X, Scelo G, Purdue MP, Rothman N, Johansson M, Ye Y, et al. A genome-wide association study identifies a novel susceptibility locus for renal cell carcinoma on 12p11.23. Hum Mol Genet 2012;21:456–62.
49. Kojima S, Enokida H, Yoshino H, Itesako T, Chiyomaru T, Kinoshita T, et al. The tumor-suppressive microRNA-143/145 cluster inhibits cell migration and invasion by targeting GOLM1 in prostate cancer. J Hum Genet 2014;59:78–87.
50. Melo SA, Kalluri R. Molecular pathways: microRNAs as cancer therapeutics. Clin Cancer Res 2012;18:4234–9.

Published OnlineFirst June 18, 2015; DOI: 10.1158/1078-0432.CCR-14-1566

Clinical Cancer Research

Identification and Functional Validation of Reciprocal microRNA–mRNA Pairings in African American Prostate Cancer Disparities

Bi-Dar Wang, Kristin Ceniccola, Qi Yang, et al.

Clin Cancer Res Published OnlineFirst June 18, 2015.

Nature Reviews Urology advance online publication 7 July 2015; doi:10.1038/nrurol.2015.161

PROSTATE CANCER

miRNA–mRNA pairs are differently expressed in African American men

Comparison of mRNA and microRNA (miRNA) expression in prostate cancer samples from African American men and American men of European descent has shed new light on the possible cause of the disparity between these two populations with regards to this disease.

Using integrative genomics, Wang and colleagues identified 22 miRNAs that are specific to prostate cancer in African American men and 18 miRNAs specific to prostate cancer in European Americans. Moreover, comparison of miRNA expression between the two populations showed 10 miRNAs are significantly enriched or depleted in samples from African American men compared with European American men.

Further analysis identified 150 reciprocally expressed miRNA–mRNA pairings and 124 Kyoto Encyclopedia of Genes and Genomes (KEGG) pathways significantly associated with prostate cancer in African American men. These pathways included ERBB, MTOR, WNT, JAK–STAT, TGF-β, P53 and VEGF. Most notably, genes associated with the ERBB pathway were upregulated in prostate-cancer samples from African American men and downregulated in samples from European American men.

> “...10 miRNAs are significantly enriched or depleted...”

Mapping population-associated miRNA–mRNA pairings on to the ERBB signalling pathway revealed 17 specific, two enriched and four depleted African-American miRNAs predicted to target 56 of 85 ERBB signalling genes and also 14 novel miRNA–mRNA pairs. Dr Norman Lee, principle investigator, told *Nature Reviews Urology* “Disrupting miRNA–mRNA pairings resulted in a less tumorigenic phenotype in African American prostate cancer cell lines, with the opposite effect observed in European cancer cell lines, suggesting a molecular basis for prostate cancer disparities among different populations.” Dr Bi-Dar Wang, lead author, added “The expression profiles of miR-133a–*MCL1*, miR-513c–*STAT1*, miR-96–*FOXO3A*, miR-145–*ITPR2* and miR-34a–*PPP2R2A* pairings may serve as indicators for evaluating prostate cancer aggressiveness in patients, especially in the African-American population”, concluding, “A patient’s ethnic background could be an important factor in future clinical studies assessing the efficacy of EGFR, PI3K, ATK and/or mTOR inhibitors.”

Louise Stone

Original article Wang, B.-D. *et al*. Identification and functional validation of reciprocal microRNA–mRNA pairings in African American prostate cancer disparities. *Clin. Cancer Res*. doi:10.1158/1078-0432.CCR-14-1566